Novel replication-competent reporter-expressing Rift Valley Fever Viruses for molecular studies.

Aitor Nogales[a,*, #] 0000-0002-2424-7900, Celia Alonso[a, 0009-0009-9661-3226*], Sandra Moreno[a 0000-0002-3548-037X], Gema Lorenzo[a 0000-0003-1869-9051], Belén Borrego[a 0000-0002-0801-9166], Luis Martinez-Sobrido[b 000-0001-7084-0804], Alejandro Brun[a, #] 0000-0001-7865-538X.

[a]*Centro de Investigación en Sanidad Animal (CISA), Instituto Nacional de Investigación y Tecnología Agraria y Alimentaria, Consejo Superior de Investigaciones Científicas (INIA-CSIC), Valdeolmos, 28130 Madrid, Spain*

[b]*Texas Biomedical Research Institute, San Antonio, TX, United States.*

**Contributed equally.*

[#]Corresponding authors.

Running Head: Rift Valley fever viruses expressing reporter genes

[#]Address correspondence to Alejandro Brun, brun@inia.csic.es.

ABSTRACT

Rift Valley fever virus (RVFV) is a mosquito-borne zoonotic disease that causes severe disease in both domestic and wild ungulates and humans, making it a significant threat to livestock and public health. The RVFV genome consists of three single-stranded, negative-sense RNA segments differing in size: Small (S), Medium (M) and Large (L). Segment S encodes the virus nucleoprotein N and the virulence-associated factor non-structural (NSs) protein in opposite orientations, separated by

an intergenic region (IGR). To overcome the current need of using secondary techniques to detect the presence of RVFV in infected cells, we used T7-driven polymerase plasmid-based reverse genetics to generate replication-competent recombinant (r)RVFV expressing Nanoluciferase (Nluc) or Venus fluorescent proteins. These reporter genes were used as valid surrogates to track the presence of RVFV in mammalian and insect cells. Notably, we explored the genome plasticity of RVFV and compared four different strategies by modifying the viral segment S in order to introduce the reporter gene foreign sequences. The reporter-expressing rRVFV were stable and able to replicate in cultured mammalian and insect cells, although to a lesser extent than the recombinant wild-type (WT) counterpart. Moreover, rRVFV expressing reporter genes were validated to identify neutralizing antibodies or compounds with antiviral activity. *In vivo*, all mice infected with the reporter-expressing rRVFV displayed an attenuated phenotype, although at different levels. These rRVFV expressing reporter genes provide a novel approach to better understand the biology and pathogenesis of RVFV, and represent an excellent biotechnological tool for developing new therapeutics against RVFV infections.

IMPORTANCE

Rift Valley fever virus (RVFV) is a mosquito-borne virus and zoonotic agent threat that can be deadly to domestic or wild ungulates, and humans. In this work, we used reverse genetics approaches to explore the genome plasticity of RVFV by generating a set of recombinant rRVFV that express fluorescent or luminescent proteins to track viral infection. All the generated reporter-expressing rRVFV were able to propagate in mammalian or insect cells, and in a mouse model of infection. Our studies may contribute to advances in research on RVFV and other bunyaviruses and

pave the way for the development of novel vaccines and the identification of new antivirals for the prophylactic and therapeutic treatment, respectively, of RVFV infections.

KEY WORDS: Rift valley fever virus (RVFV), segment S, reporter gene, NanoLuc luciferase, Venus fluorescent protein, neutralizing antibody, antiviral, mouse model.

INTRODUCTION

Rift Valley fever (RVF) is a re-emerging zoonotic disease endemic to Africa, the Middle East, and the Indian Ocean with recurrent outbreaks in domestic or wild ruminants resulting in spillover into humans (1-3). Rift Valley fever virus (RVFV) is a phlebovirus belonging to the family *Phenuiviridae* that is transmitted by *Aedes* and *Culex* mosquito species, but may also be transmitted through direct contact with body fluids of infected animals (2). Human infections in endemic regions are usually asymptomatic or can cause mild illness. However, in some cases, infected persons develop more severe symptoms that range from ocular lesions to encephalitis and haemorrhagic fever or death (1). Moreover, RVF disease leads to high abortion rates in herds and neonatal mortality, making it a significant threat to livestock of affected regions (4). Due to its virulence, economic impact and lack of efficient vaccines or antivirals, RVFV is considered a potential biothreat and is listed as a select agent by both the U.S. Health and Human Services (HHS) and the U.S. Department of Agriculture (USDA). In addition, RVFV is included in the World Health Organization (WHO) Blueprint list of pathogens that are prioritised for research and development of countermeasures (5). Therefore, research to better understand RVFV pathogenesis

75 and to develop effective prophylactic vaccines and therapeutic strategies is urgently
76 needed for the control of this important human viral pathogen.

77 RVFV virions are icosahedral and contain a lipid envelope enclosing a
78 nucleocapsid. The viral genome is formed by three single-stranded RNA segments
79 with negative and ambisense polarity and different sizes: the large (L), medium (M),
80 and small (S) (6, 7). The 3′ and 5′ ends of the coding regions contain regulatory
81 untranslated regions (UTRs). The L segment encodes the RNA-dependent RNA
82 polymerase (RdRp) (8, 9). The M segment encodes a polyprotein, which, upon
83 protease processing, gives the two membrane glycoproteins (Gn and Gc) that form
84 heterodimers in the viral envelope (10-13), and a non-structural protein (NSm)
85 involved in modulation of apoptosis (14). The mRNA of the M segment may also
86 translate an additional 78 kDa protein via the NSm and Gn open reading frames
87 (ORFs) (15). The S segment encodes the virus nucleoprotein (N) and the virulence-
88 associated factor non-structural (NSs) protein in opposite orientations, separated by
89 an intergenic region (IGR) (16-18). Together with the viral RNA, the N and RdRp
90 proteins constitute the viral replication complex. While the genomic L and M RNAs
91 serve as templates for the synthesis of their cognate antigenomic RNAs and mRNAs,
92 the segment S uses an ambisense coding strategy for the expression of N and NSs
93 proteins in opposite orientation. The genomic S segment serves as a template for the
94 synthesis of N mRNA and the antigenomic S segment serves as the template for the
95 synthesis of NSs mRNA.

96 Reverse genetics methods have provided researchers with a powerful
97 experimental approach for generating recombinant RVFV (rRVFV), which have
98 allowed researchers to study important aspects of the biology and replication of RVFV,
99 identify host factors, study markers of pathogenesis, and generate live-attenuated

100 vaccines (19-28). The generation of reporter-expressing rRVFV has been described
101 previously and engineered to contain four-segments: an authentic L segment, an S
102 segment that encodes N and enhanced green fluorescent protein (eGFP), and two M-
103 type segments that encode either NSmGn or Gc (29). This rRVFV-4s eGFP was able
104 to reach high titters in mammalian BSR cells, but not in insect C6/36 cells (29).
105 Moreover, the virus was highly attenuated in mice (29). In addition, the generation of
106 rRVFV lacking NSs (ΔNSs) expressing either eGFP or firefly luciferase (FLuc) in place
107 of NSs have also been described (22). The growth curves of recombinant wild-type
108 (WT) and ΔNSs-eGFP or ΔNSs-FLuc were similar in Vero cells, but the growth of the
109 reporter viruses in mice was highly attenuated compared to their WT counterpart (22).
110 Moreover, while the eGFP sequence was well tolerated in the viral genome, FLuc
111 sequence was unstable when expressed by the rRVFV (22).

112 In this work we used a new experimental strategy to generate replication-
113 competent, reporter-expressing rRVFV in which heterologous genes are inserted into
114 the viral genome without the need for segment duplication or gene deletion. Notably,
115 we used four different approaches that also provided information related to the
116 genome plasticity of RVFV. While numerous reporter genes with different features
117 have been described, fluorescent and bioluminescent proteins are becoming the
118 preferred choice for researchers due to their high sensitivity and the continuous
119 improvement of the technologies associated with their detection (30-34). Therefore,
120 we have generated a set of rRVFV expressing fluorescent (Venus) or nanoluciferase
121 (Nluc) reporter genes. All viruses were characterized *in vitro* and *in vivo* and proven to
122 be a valid method for studying viral replication and propagation or for the identification
123 of antivirals and neutralizing antibodies (NAbs).

124

125 **RESULTS**

126 **Generation of replication-competent rRVFV expressing reporter genes**

127 To generate replication-competent, reporter-expressing rRVFV (strain 56/74),
128 the sequence of Nluc or Venus and the porcine teschovirus 1 (PTV-1) 2A
129 autoproteolytic cleavage site were cloned upstream or downstream of the ORF of the
130 N or NSs proteins in the segment S (**Figure 1**). We chose Nluc due to its small size
131 (~20 kDa), stability, and brightness (30, 35). The fluorescent protein Venus
132 (~26,8 kDa) was also selected because of the intensity of the signal and previous
133 experience with other RNA viruses, where the insertion of Venus and Nluc in the
134 genome was well tolerated (36-39). Importantly, the UTRs and the IGR of the S
135 segment were not modified. We then used T7-pol plasmid-based reverse genetics
136 approaches to generate a set of rRVFV expressing Nluc or Venus at different genome
137 positions. Notably, 4 Nluc-expressing rRVFV, covering the 4 strategies used, were
138 recovered, namely Nluc2ANSs, NSs2ANluc, N2ANluc, and Nluc2AN. However, only
139 3 Venus-expressing rRVFV were rescued: Venus2ANSs, NSs2AVenus, and
140 Venus2AN (**Figure 1**). We were not able to successful rescue the N2AVenus even
141 after multiple attempts. Moreover, a rRVFV WT (rWT) was also generated for
142 comparison.

143

144 **Growth properties and plaque phenotype of reporter-expressing rRVFV in**
145 **mammalian cells**

146 We next evaluated the fitness of Nluc-expressing (**Figures 2A and B**) or
147 Venus-expressing (**Figures 2C and D**) rRVFVs in mammalian cells by assessing their
148 growth properties and compare them to those of rWT. To this end, confluent
149 monolayers of Vero E6 cells were infected with the different viruses at the same

150 multiplicity of infection (MOI; 0.01), and the presence of virus in culture supernatants
151 was quantified at different times post-infection (p.i).

152 Replication of Nluc-expressing rRVFVs was delayed and did not reach titters
153 similar to those of the rWT (**Figure 2A**). Moreover, higher replication levels were
154 observed when Nluc was inserted next to the UTRs (Nluc2AN and Nluc2ANSs),
155 instead of next to the IGR (N2ANluc and NSs2ANluc) and when the reporter gene was
156 fused to the NSs ORF (Nluc2ANSs and NSs2ANluc) instead of the N ORF (Nluc2AN
157 and N2ANluc) (**Figure 2A**). In addition, Nluc activity in culture supernatants was
158 evaluated at the same time points (**Figure 2B**). Nluc activity increased in a time-
159 dependent manner, peaking at 72 h p.i. (the last time point evaluated in our study),
160 most likely because the cytopathic effect (CPE) caused by the viral infection resulted
161 in the release and accumulation of Nluc in the cell culture supernatants. Interestingly,
162 viruses expressing Nluc in the same ORF that the viral N gene (Nluc2AN and
163 N2ANluc) displayed higher levels of Nluc activity (**Figure 2B**). This is most likely
164 because of the higher levels of N expression during viral infection as compared to NSs
165 (40).

166 Similarly, the viral growth of Venus-expressing rRVFVs was delayed as
167 compared with that of rWT, and the replication of Venus2AN was more affected than
168 the replication of Venus2ANSs (**Figures 2C and D**). Venus expression was detected
169 as early as 24 h p.i. and steadily increased, in a time-dependent manner, until 72 h
170 p.i., when visualization was reduced due to the virus-induced CPE. Importantly, all
171 reporter-expressing rRVFVs were still able to reach high viral titters in culture
172 supernatants (~$10^{5/6}$ PFU/ml) but in all cases were reduced as compared to rWT (~10^{7}
173 PFU/ml) (**Figure 2**). Our data suggest that the insertion of Nluc in the viral genome is
174 better tolerated than the insertion of Venus. In addition, our results also provide some

175 clues regarding the regions of RVFV segment S that can be more suitable for the
176 expression of foreign sequences. Therefore, results indicate that reporter-expressing
177 rRVFVs may be used to track and quantify the dynamics of viral infection in vitro by
178 using either fluorescent or luciferase reporter genes.

179 We also evaluated the plaque phenotype of the rRVFVs in Vero E6 and
180 compared it to the rWT virus (**Figure 3**). For that, Vero E6 cells were infected and at
181 72 h p.i., immunostaining using specific antibodies against Nluc or GFP (for Venus
182 detection), and crystal violet staining. As expected, we detected Nluc or Venus-
183 positive viral plaques only in cells infected with Nluc- or Venus-expressing rRVFVs,
184 respectively. In addition, all the Nluc- or Venus-positive plaques colocalized with the
185 plaques detected by crystal violet staining, confirming that all the rRVFV-infected
186 plaques expressed the Nluc or Venus reporter gene. Moreover, plaque sizes were in
187 agreement with viral replication kinetics (**Figure 2**), since the sizes of the viral foci
188 produced by reporter-expressing rRVFVs were smaller than those of the produced by
189 the rWT virus (**Figure 3**), most likely due to the effect of the reporter gene on viral
190 fitness. Overall, these data and our previous studies with other reporter-expressing
191 replication-competent viruses (36, 38, 41, 42) demonstrate that Nluc and Venus can
192 be successfully expressing from the viral genome using the PTV-1 2A site, and
193 reporter gene expression can be used as valid surrogates to monitor viral infection
194 without the need for secondary approaches to detect the presence of the virus in
195 infected cells, or the presence of virus in culture supernatants.

196

197 **Analysis of protein expression in cells infected with reporter-expressing rRVFVs**

198 To assess the expression of Nluc and Venus, confluent monolayers of Vero E6
199 cells were mock-infected or infected with rWT and Nluc-expressing rRVFVs (**Figure**

200 **4A**) or Venus-expressing rRVFVs (**Figure 4B**). Then, the cells were analyzed by
201 indirect immunofluorescence microscopy and confocal microscopy, using antibodies
202 against RVFV (detecting Gn/Gc and N viral proteins), Nluc (**Figure 4A**), or GFP (for
203 Venus detection) (**Figure 4B**). As expected, only rRVFV-infected cells were stained
204 with the anti-RVFV polyclonal antibody (pAb). Accordingly, the expression of Nluc and
205 Venus was detected only in cells infected with Nluc- (**Figure 4A**) or Venus-expressing
206 (**Figure 4B**) rRVFVs, respectively. Interestingly, Nluc was detected in the cytosol
207 resembling the characteristic intranuclear NSs filaments in both Nluc2ANSs and
208 NSs2ANluc viruses, suggesting that the cleavage efficiency of the 2A peptide
209 sequence selected was not 100%, as previously described (43, 44) and shown in
210 figure 5. In contrast, the Nluc signal colocalizes along the RVFV signal in the
211 cytoplasmic compartment in cells infected with either N2ANluc or Nluc2AN viruses,
212 most likely in these cells some fraction of Nluc is also colocalizing with the viral N
213 protein. The presence of intranuclear NSs accumulation was barely detectable in both
214 NSs2AVenus and Venus2ANSs viruses in which both RVFV and Venus signals
215 colocalize in the cytoplasmic compartment as of Venus2AN virus.

216 Next, protein expression in Vero E6 cells was evaluated by Western blot at 24
217 and 48 h p.i. (**Figure 5**). Total cell extracts from either mock-, rWT-, or reporter-
218 expressing rRVFV-infected Vero E6 cells were tested using antibodies specific for
219 RVFV, N or NSs, Nluc (**Figure 5A**) or Venus (**Figure 5B**) reporters, and for the loading
220 control, actin. Western blot analysis revealed specific bands corresponding to the
221 expected molecular sizes of the viral Gn (54 kDa) and Gc (56 kDa), N and NSs
222 proteins. The N protein expressed by N2ANluc virus displays a slightly higher
223 molecular mass as a consequence of the proteolytic mechanism that leaves the linker
224 and part of the 2A peptide sequence at the C-term of the fusion partner. Interestingly,

225 this shift is also observed for NSs (NSs2ANluc) although only at 24 h p.i. In addition,
226 we observed specific bands for Nluc or the fusion protein of Nluc with NS or N (**Figure**
227 **5A**) and for Venus or the fusion protein Venus with NS or N (**Figure 5A**), indicating
228 that the proteolytic efficiency of the 2A peptide sequence used was not 100%, as
229 previously described (43, 44). Moreover, protein expression was greater at 48 h p.i. In
230 the case of cell extracts infected with Venus-expressing rRVFVs, we also observed
231 bands of lower molecular size than expected, which could indicate Venus degradation.
232 A pathway by which RVFV NSs blocks the host antiviral responses of infected
233 cells is the degradation of cellular proteins such as protein kinase R (PKR) (45-47). In
234 order to determine whether our gene modifications affected the ability of modified NSs
235 to degrade PKR and therefore be responsible of viral attenuation, HEK293T cells were
236 infected with rRVFV expressing the reporter gene in the NSs locus (Nluc2ANSs,
237 NSs2ANluc, Venus2ANSs, and NSs2AVenus), and whole cell extracts were analyzed
238 by Western blot (**Figure 5C**). In all infected cells, the expression of PKR was reduced,
239 suggesting that the viral NSs is functional in all cases or at least its ability to degrade
240 PKR was not impaired.
241
242 **Intracellular *vs* extracellular activity of Nluc and analysis of intracellular Venus**
243 **expression**
244 To determine whether differences in Nluc activity in cell culture supernatants
245 were due to differences in the levels of Nluc secretion *versus* its accumulation in
246 infected cells, confluent monolayers of Vero E6 cells were infected (MOI of 0.01) with
247 Nluc-expressing viruses, and the presence of virus in culture supernatants was
248 evaluated at 48 h p.i. (**Figure 6A**). In addition, Nluc activity in the supernatant or in cell
249 extracts was quantified (**Figure 6B**). There was a correlation between Nluc activity in

250 the supernatants and that in the cell extracts, suggesting that differences in Nluc
251 activity were not a consequence of a greater secretion into the supernatant or cell
252 accumulation of Nluc; indeed, these differences were most likely due to differences in
253 the Nluc position in the viral genome. However, the observed intranuclear detection of
254 Nluc aggregates (**Figure 4**), resembling NSs filamentous structures, might correlate
255 with lower availability of soluble Nluc in cells infected with the NSs2ANluc expressing
256 virus.

257 Next, Vero E6 cells infected with Venus-expressing rRVFVs were evaluated by
258 flow cytometry to quantify the percentage of cells expressing Venus, N protein, or
259 Venus and N protein at 24 h. p.i, using the anti N monoclonal antibody (mAb)
260 2B1conjugated to Alexa 674 (**Figure 6C**). Notably, the percentage of Venus+ cells
261 was greater than the percentage of N+ cells. Moreover, 100% of the Venus+ cells
262 were also N+. In contrast, and as expected, the rWT infection control was detected
263 only after N staining. Our data indicate that the expression of Venus during viral
264 infection could be a more sensitive method than antigen staining to detect the
265 presence of the virus in infected cells, even more than detecting one of the highly
266 expressed proteins during viral infection (e.g. N), at least, at early times post infection.
267

268 ***In vitro* stability of the reporter-expressing rRVFV**

269 The genetic stability of reporter-expressing viruses is important for their use
270 since can limit some of their applications (36, 38). Therefore, we evaluated the *in vitro*
271 stability of all the reporter-expressing rRVFVs generated (**Figure 7**). To that end, Nluc-
272 or Venus-expressing rRVFVs were passaged in duplicate three consecutive times in
273 Vero E6 cells, and the percentage of reporter-expressing viruses was determined by
274 plaque assay. In the case of Venus-expressing viruses, plaques were observed

275 directly under a fluorescence microscope. To test the expression of Nluc, plaques
276 were amplified in 96-well plates, and then, Nluc activity in the cell culture supernatant
277 was evaluated at 48 h.p.i. rRVFVs that express Nluc or Venus were 100% stable at
278 passage two (virus working stock) and passage 3 (first amplification passage) in all
279 cases. Interestingly, the rRVFVs expressing the reporter genes close to the IGR
280 (NSs2ANluc, N2ANluc, and NSs2AVenus) were more stable than the viruses
281 encoding Nluc or Venus next to the UTRs (Nluc2ANSs, Nluc2AN, and Venus2ANSs),
282 where a gradual loss of Nluc or Venus expression was observed from passages 5 or
283 4, respectively (**Figure 7**). Venus2AN was an exception since it expressed stable
284 fluorescent levels up to 5 passages.
285

286 **Use of rRVFV expressing Nluc for the identification of antivirals**

287 Identification of compounds that inhibit RVFV normally requires the use of
288 secondary approaches to evaluate viral infection (48-51). The use of reporter-
289 expressing viruses compatible with high-throughput screening for the identification of
290 antivirals may be an interesting alternative to traditional assays. To demonstrate that
291 Nluc-expressing rRVFVs are a valid surrogate for identifying antivirals, we examined
292 the ability of ribavirin to inhibit RVFV infection using the Nluc-expressing rRVFVs
293 NSs2ANluc, Nluc2ANSs, and Nluc2AN (**Figures 8A and B**). We did not include the
294 virus N2ANluc in the assay, because this rRVFV was the most affected in viral
295 replication (**Figure 2**). At high concentrations of ribavirin (starting concentration of
296 1000 μM), all Nluc-expressing rRVFV were inhibited in a dose-dependent manner, as
297 determined by Nluc activity in cell culture supernatants (**Figure 8A**). Importantly, the
298 IC_{50} values were similar for all the viruses tested (**Figure 8B**) and consistent with those
299 described in the literature (48-52).

300

301 **Use of rRVFV expressing Nluc for the identification of NAbs**

302 NAbs are a key immunological outcome for the induction of protective immunity
303 after vaccination to prevent RVFV infections. Similar to the previously described
304 antiviral test, viral neutralization assays typically involve the use of secondary methods
305 to measure viral infection. Because the presence of Nluc in the culture supernatants
306 is a valid surrogate of viral replication, an Nluc-based microneutralization assay was
307 developed using the Nluc-expressing rRVFVs. Confluent monolayers of Vero E6 cells
308 were infected with Nluc-expressing rRVFV, which had previously been incubated with
309 sheep sera obtained before or at 14 days post-vaccination with an experimental RVFV
310 vaccine (20) (**Figures 8C and D**). Then, at 48 h p.i. Nluc activity in the culture
311 supernatants was quantified (**Figure 8C**). As expected, all viruses were neutralized,
312 in a dose-dependent matter, by sera collected at 14 days post-vaccination. Using
313 sigmoidal dose-response curves, we determined the 50% neutralization titter (NT_{50})
314 obtained by the quantification of Nluc (**Figure 8D**). Importantly, the NT_{50} was similar
315 for all the tested viruses. These data indicate that our Nluc-based-microneutralization
316 assays may be a suitable method for the rapid identification and quantification of
317 antivirals and NAbs.

318

319 **Growth properties of rRVFV in C6/36 mosquito cells**

320 RVFV is an arbovirus, with mosquitoes playing an important role in the natural
321 transmission cycle. Therefore, the growth properties of the reporter-expressing
322 rRVFVs were also investigated in the *Aedes albopictus* clone mosquito larvae derived
323 cell line (**Figure 9**). For that, C6/36 cells were infected (MOI; 0.01) with the different
324 viruses, and the presence of virus in culture supernatants was quantified at 3, 5 and 7

325 days p.i. As expected, we observed differences in the levels of viral replication among
326 the rRVFVs. Nluc-expressing rRVFVs replicated to a lesser extent than the rWT. In
327 addition, as previously observed in Vero E6 cells (**Figure 2**), higher replication levels
328 were observed when Nluc was cloned in the ORF of the NSs gene (Nluc2ANSs vs
329 Nluc2AN or NSs2ANluc vs N2ANluc) (**Figure 9A**). Furthermore, the presence of Nluc
330 in cell culture supernatants was measured at the same time points. Nluc activity
331 increased in a time-dependent manner, peaking at 7 days p.i. (the last time point
332 evaluated). Similar to Vero E6 cells, viruses expressing Nluc from the ORF of the viral
333 N gene displayed also high levels of Nluc activity, most likely because of the higher
334 levels of N expression during viral infection than NSs (40) (**Figure 9B**). In contrast to
335 what was detected in Vero E6, the NSs2ANluc virus also had high Nluc activity level.
336 The viral replication of Venus-expressing rRVFVs was also delayed as compared with
337 that of the rWT (**Figure 9C and D**). Venus expression was detected as early as 3 days
338 p.i. (first time point evaluated) and steadily increased in a time-dependent manner,
339 until 7 days p.i. (last time point evaluated). Therefore, the data indicate that Nluc- and
340 Venus-expressing rRVFVs may also be used to track the dynamics of viral infection in
341 mosquito cells.
342
343 **Pathogenicity and replication of Nluc-expressing rRVFV in mice**
344 Next, we evaluated the pathogenicity of Nluc-expressing rRVFV in BALB/C
345 mouse model of infection (**Figure 10**). To that end, groups of mice (n = 5) were
346 inoculated intraperitoneally with 10^3, 10^4 or 10^5 PFU of each rRVFV and body weight
347 loss (**Figure 10A**) and survival (**Figure 10B**) were monitored for 18 days. Compared
348 with rWT-infected mice, Nluc-expressing rRVFVs were attenuated. With a lower dose
349 of 10^3 PFU, all mice inoculated with rWT lost weight and all of them succumbed to viral

350 infection. However, only rRVFV NSs2ANluc displayed virulence level comparable to
351 the rWT, and although moderate body weight loss occurred between days 7 and 9,
352 four of the 5 mice died. When animals were infected with 10^4 PFU, only two of five
353 mice inoculated with rWT died, and none of the mice infected with the Nluc-expressing
354 rRVFVs showed signs of morbidity and all of them survived viral infection.
355 Interestingly, with the higher dose of 10^5 PFU, three animals inoculated with rWT and
356 2 inoculated with rRVFV Nluc2ANSs succumbed to the infection, although without
357 significant body weight loss. The absence of a correlation between the dose and
358 virulence was somehow expected, since this phenomenon has been shown before for
359 RVFV (53, 54), including some of our studies (data not shown).

360 Given that RVFV is isolated from blood and causes viremia, it was speculated
361 that the presence of Nluc could be detected in blood samples from infected mice, as
362 occurs with Nluc-expressing bluetongue virus, which is also isolated from blood
363 samples of infected mice (38). To prove this, Nluc activity was measured in plasma
364 samples from infected animals and days 3 and 5 p.i. However, Nluc activity was not
365 detected in any of the plasma samples (data not shown), even presence of the virus
366 was detected at the same times post-infection by qRT-PCR (**Figure 10C**). Replication
367 levels were higher at 3 days p.i in all cases and a clear correlation between mortality
368 and leves of viral RNA in blood was not observed (**Figure 10C**). To study
369 seroconversion in the animals, serum samples were collected at 18 d p.i, and the
370 presence of antibodies against RVFV N was analyzed by ELISA (**Figure 10D**). The
371 presence of anti-N antibodies is typically used as a sign of infection and replication
372 and as a valid serological diagnostic method (20, 55-58). We observed seroconversion
373 in all the mice that survived infection (**Figure 10D**), suggesting that Nluc-expressing
374 rRVFVs were able to replicate, although they are mostly attenuated in vivo. Altogether,

375 these data indicate that the S segment-based reporter gene expression strategy
376 contributes to in vivo attenuation depending on the insertion position, at least in the
377 mouse model of infection used.
378

379 **DISCUSSION**

380 The establishment of reverse genetics systems for RVFV and other
381 bunyaviruses has allowed researchers to investigate virus replication, mechanisms of
382 viral pathogenesis, and the generation of live-attenuated vaccines (7, 17, 19, 45, 56,
383 59). Reporter-expressing, replication-competent rRVFV represents a powerful tool for
384 basic and/or translational studies (9, 19, 22, 29). Previously, reporter-expressing
385 rRVFVs were generated using a four segment strategy or by substituting the viral NSs
386 sequence with the reporter gene (22, 29). In this work, we have assayed the insertion
387 of a reporter gene at four different positions in the viral segment S, avoiding duplication
388 of viral segments or removal of non-structural viral genes; and, therefore, representing
389 a more biological approach than previous strategies. In this new approach, foreign
390 sequences were expressed from the same viral N or NSs ORFs using the PTV-1 2A
391 cleavage site, an approach that has been successfully implemented for the
392 development of other replication-competent, reporter-expressing viruses with high
393 success (38, 43, 44). Similar to these previous studies, we have been able to
394 successfully rescue using this novel 2A approach RVFV expressing fluorescent and
395 luciferase reporter genes. Based on the different properties of fluorescent and
396 luciferases proteins (31-34, 36) it is important to carefully considered the advantages
397 and disadvantages of these reporter genes before performing experiments. For
398 example, *in vitro*, luciferases may be more appropriate for quantitative determinations
399 (33, 35, 60). Conversely, fluorescent proteins are a better choice to observe

400 localization in live cells (31, 32). Thus, in this manuscript we used the same innovative
401 approach to generate rRVFVs expressing luciferase (Nluc) or fluorescent (Venus)
402 reporter proteins. However, other reporter luciferase or fluorescent proteins can be
403 inserted into the genome of RVFV using the same experimental strategy to rescue
404 similar viruses. Moreover, based on the results obtained in this study, we have been
405 able to have a better understanding on the plasticity of the RVFV genomic S segment
406 to accommodate extra foreign sequences and how that influences expression levels
407 of foreign proteins or viral attenuation of recombinant viruses expressing these
408 reporter genes from the locus of the viral N or NSs ORFs.

409 Subsequently, the expression of the Nluc and Venus was confirmed, and the
410 virological phenotypes of Nluc- and Venus-expressing viruses were characterized. As
411 expected, the infection of mammalian Vero E6 or mosquito C6/36 cells with reporter-
412 expressing rRVFV was visualized in real time without the need for secondary methods.
413 Moreover, the expression of Venus and Nluc revealed similar kinetics that correlated
414 with the levels of viral replication, further demonstrating the feasibility of using Nluc or
415 Venus as valid surrogates of viral replication and infectivity without the need of
416 secondary approaches to identify the presence of the virus in infected cells or cell
417 culture supernatants, respectively. Compared to rWT, replication of the reporter-
418 expressing rRVFVs was affected, although, in general, all viruses growth with high
419 viral titers. Importantly, all the rRVFVs were stable during multiple passages in cell
420 culture, which is desirable for studies using reporter-expressing viruses (36, 38, 41).
421 However, we identified differences regarding the strategy used to insert the reporter
422 genes (**Table 1**). Greater expression was observed when reporter genes were
423 expressed from the locus of the viral N protein. On the other hand, rRVFV encoding
424 Nluc or Venus from the locus of the NSs protein replicated to a greater extent but had

425 reduced levels of reporter gene expression. Notably, if reporter genes were inserted
426 after the UTR sequence, we observed higher viral titers than those of recombinant
427 viruses expressing the reporter gene before the UTR sequence. However, the
428 mechanisms responsible for these differences remain to be investigated and will be
429 the subject of our follow up studies aimed to assess foreign gene expression from the
430 RVFV S segment based on their location in the viral genome.

431 Notably, we developed and validated a Nluc-based microneutralization assay
432 that allow us to rapidly identify antiviral compounds and NAbs against RVFV. Our
433 novel reporter-based mincroneutralization assay represent an excellent option to
434 interrogate large libraries of compounds or antibodies to identify those with antiviral
435 and neutralizing activity against RVFV, including their feasibility to implement in high-
436 throughput (HTS) approaches to rapidly and sensitivity screen for novel antivirals or,
437 in the case of NAbs, the efficacy of novel vaccine candidates. In addition, the virulence
438 of Nluc-expressing rRVFVs was assessed in BALB/C mice. In this mouse model of
439 infection, reporter-expressing viruses were attenuated as compared to rWT, and
440 mortality was only observed in mice inoculated with Nluc2ANSs or NSs2ANluc viruses.
441 Importantly, all reporter rRVFVs were able to replicate in this mouse model. However,
442 the reporter rRVFVs could display a more virulent phenotype in other mouse strains
443 that are more susceptible to RVFV infection (61). It has been shown that BALB/C mice
444 (used in our study) are slightly more resistant than other mouse strains, where different
445 disease phenotypes (hepatic, neurological and mixed) can be clearly distinguished
446 (53, 54, 62). In addition, differences depending on the sex and age of the animals have
447 been reported, with males being more susceptible than females (63, 64). However, in
448 our study, we have used only female BALB/C mice, and the phenotype of our rRVFV
449 in other mouse models or in male vs female animals remains unknown. Interestingly,

450 all mice produced anti-N antibodies, suggesting that the viruses were able to infect
451 and replicate (20, 55-58), although causing limited or no pathogenicity in terms of body
452 weight loss or mortality. Altogether, our results indicate that additional studies to
453 determine the best mouse strain, sex and viral dose should be taken into account
454 when using the generated reporter-expressing rRVFV.

455 NSs is localized both in the cytoplasm and nucleus of infected cells and it is
456 considered the major virulence factor of RVFV. NSs form nuclear filamentous
457 structures through homo-oligomerization (65) and inhibit host innate immune
458 responses through different strategies, including inhibition of the type I interferon (IFN)
459 system (66), and induction of host cellular transcription shut-off (67). It has been
460 suggested that NSs filament formation is dispensable for efficient replication in vitro
461 and appears to be important but insufficient for virulence in vivo (68). In two of our
462 strategies used to generate reporter-expressing rRVFVs, we introduced the foreign
463 sequence adjacent to the NSs sequence. This could affect some of the antiviral
464 functions of NSs, including the formation of filamentous structures, and thus explain
465 the attenuated phenotype in vivo. However, filament like structures resembling those
466 of WT NSs were clearly observed in the virus expressing NSs2ANluc and to a lesser
467 extent in the Nluc2ANSs virus. Interestingly, the detection of such filaments was
468 accomplished using an anti-Nluc antibody, indicating that unprocessed NSs-Nluc or
469 Nluc-NSs fused proteins were transported to the nucleus of the infected cells. How
470 this fact correlates with the observed virulence levels in vivo of both rRVFVs remains
471 to be elucidated. In addition, it could be interesting, to compare the viral fitness and
472 attenuation of the described rRVFV encoding the reporter gene in the NSs side with a
473 rRVFV lacking the viral NSs gene.

474 The formation of the RVFV N-RNA complex protects the vRNA and replication
475 intermediates from nucleases and is key for viral replication-transcription, and efficient
476 packaging of the viral genome (69, 70). It has been observed in crystallographic
477 structures that the N protein adopts two major conformations, open and closed (69,
478 71-73). It cannot be discarded that by inserting the reporter gene next to the viral N
479 sequence, the proper function of the N protein during viral infection could be affected,
480 due to the intrinsic proteolytic mechanism of the PTV-2A peptide in which the cleavage
481 site lies between the Gly-Pro bond at the end of the peptide, therefore 21 extra amino
482 acids are added to the end of the viral nucleoprotein. This could explain the observed
483 attenuation in vivo and reduced viral fitness in vitro compared with those of the rWT
484 or with rRVFVs expressing the reporter gene on the NSs side.

485 In addition, although the UTRs and IGR of the viral segment S were not directly
486 modified in our strategy, the insertion of foreign sequences could introduce some
487 changes in the RNA structure or unknown cis-regulatory sequences of the viral
488 genomic and/or antigenomic sequences. In fact, it was observed, that reporter-
489 expressing rRVFVs containing the reporter gene next to the 5´ or 3´ UTRs displayed
490 better fitness than viruses in which the heterologous genes were inserted next to the
491 IGR (17, 74-76). Notably, our strategy could also be useful for developing and testing
492 novel live RVFV vaccines or vaccine vectors with different degrees of attenuation.

493

494 **MATERIALS AND METHODS**

495 **Cell lines and viruses**

496 Vero E6 cells (ATCC/CRL/1586) were routinely maintained in Dulbecco's
497 modified Eagle's medium (DMEM) supplemented with 5% fetal bovine serum (FBS),
498 1% 100x nonessential amino-acids, 100 U/mL penicillin, 100 µg/mL streptomycin, and

499 2 mM L glutamine. The cells were incubated at 37°C in the presence of 5% CO_2. BSR-
500 T7 cells (38, 77) stably expressing the bacteriophage T7 RNA polymerase were
501 maintained in the same manner as above except for the addition of 1 mg/mL of
502 Geneticin every 2-3 passages. C6/36 *Aedes albopictus* cells (ATCC CRL–1660) were
503 grown in Eagle's Minimum Essential Medium (MEM) supplemented with 10% fetal calf
504 serum (FCS), L-glutamine (2 mM), gentamicin (50 µg/ml), and MEM vitamin Solution
505 (Sigma) at 28°C.

506 The sequence of the WT South African RVFV strain 56/74 (parental virus),
507 which was used for the synthesis of the reverse genetic system, was previously
508 described (78) . GenBank: OM744400.1 (segment L), OM744401.1 (segment M) and
509 OM744402.1 (segment S). Virus stocks were propagated in Vero E6 cells and titrated
510 by plaque assay as previously described (20, 55, 56). All the experiments were
511 conducted in the biological security facility of the Animal Health Research Center
512 (CISA, INIA-CSIC).

513

514 **Plasmids**

515 All pBlueScript II SK (+) reverse genetics (RG) plasmids were synthetized *de*
516 *novo* by Biomatik and designed to contain the viral cDNAs flanked upstream by a T7
517 RNA polymerase promoter sequence and downstream by the hepatitis delta virus
518 ribozyme (HDVR) and T7 RNA polymerase terminator sequences (38). To generate
519 replication-competent reporter-expressing RVFVs and study viral genome plasticity,
520 we engineered a set of recombinant modified segments S using four different
521 strategies for the cloning of reporter genes. Importantly, the 5′- and 3′- UTRs and the
522 IGR were not modified. A common heterologous sequence was designed containing
523 a linker (GSG), the porcine teschovirus-1 (PTV-1) 2A autoproteolytic cleavage site

524 (ATNFSLLKQAGDVEENPGP), and a multicloning site (AgeI/BglII/NheI) for the
525 insertion of foreign sequences (36, 38, 42). Then, the 4 master plasmids containing
526 the heterologous sequence before or after the 5′- and 3′- UTRs or the IGR were used
527 for the cloning of the Venus or Nluc reporter genes. Reporter genes were amplified by
528 PCR using specific primers containing AgeI or NheI sites. Then, the PCR products
529 and the 4 modified segment S plasmids were digested, and the reporter genes were
530 cloned using standard molecular biology techniques. Plasmid constructs were
531 confirmed by sequencing (Macrogen). Master plasmids containing the modified
532 segment S
533 -pBS-2A-N: The reporter gene without a stop codon was cloned between the 3´UTR
534 of the genomic vRNA and the N ORF. This plasmid was used to generate Venus2AN
535 and Nluc2AN viruses.
536 -pBS-N-2A: The reporter gene with a stop codon was cloned between the N ORF and
537 the IGR. This plasmid was used to generate N2AVenus and N2ANluc viruses.
538 -pBS-NSs-2A: The reporter gene with a stop codon was cloned between the NSs ORF
539 and the IGR. This plasmid was used to generate NSs2AVenus and NSs2ANluc
540 viruses.
541 -pBS-2A-NSs: The reporter gene without a stop codon was cloned between the 5´UTR
542 of the genomic vRNA and the NSs ORF. This plasmid was used to generate
543 Venus2ANSs and Nluc2ANSs viruses.
544
545 **Rescue of recombinant viruses**
546 To rescue rRVFV, monolayers of BSR-T7 cells (T25 flasks, 80% of confluence,
547 duplicates) were cotransfected with 1 µg of each of the reverse genetics plasmids
548 encoding the RVFV cDNAs using Lipofectamine 3000 (Invitrogen) in Opti-MEM I

549 reduced serum medium (Invitrogen) according to the manufacturer's instructions.
550 Twenty-four hours after transfection, the transfection mixture was replaced with 5 mL
551 of growth medium. After 72-96 h, the cell culture supernatants were collected, clarified,
552 and used to infect fresh monolayers of Vero E6 cells. Once the CPE was observed
553 (48-96 h), the medium was harvested and clarified. Clonal rRVFV were selected by
554 plaque assays, and virus stocks were propagated in Vero E6 cells, where once the
555 CPE was observed, the medium was harvested, clarified and stored at -80ºC.
556

557 **Virus growth kinetics**

558 To evaluate virus multicycle growth kinetics, confluent Vero E6 cells (12-well
559 plate format, 5 x 10^5 cells/well, triplicates) or C6/36 cells (T25 flasks, 4 x 10^6 cells/well,
560 triplicates) were infected at an MOI of 0.01. After 1 h of virus adsorption at 37°C (Vero
561 E6) or 28ºC (C6/36), the inoculum was discarded, the cells were washed, and 1.5 mL
562 (Vero E6) or 5 mL (C6/36) of growth medium was added. At the indicated times post
563 infection (24, 48, and 72 h for Vero E6; 3, 5, and 7 days for C6/36), 150 µL of the
564 supernatant was removed and stored at -80°C. Virus titers were determined in Vero
565 E6 cells by plaque assay (plaque-forming units, PFU/mL), as previously described (20,
566 55, 56, 78). The mean value and standard deviation (SD) were calculated using
567 GraphPad Prism version 8.0.1 (GraphPad Software Inc.). In addition, cells infected
568 with Venus-expressing rRVFV were imaged using a Zeiss Axio fluorescence
569 microscope (Zeiss), and the presence of Nluc in the culture supernatants was
570 quantified using Nano-Glo luciferase substrate (Promega) following the
571 manufacturer's specifications.
572

573 **Plaque assay and immunostaining**

574 Confluent monolayers of Vero E6 cells (6-well plate format, 10^6 cells/well) were
575 infected with the indicated viruses for 1 h at room temperature, overlaid with agar, and
576 incubated at 37°C. At 3 days p.i., the cells were fixed with 10% paraformaldehyde
577 (PFA), and the overlays were removed. The cells were then permeabilized (0.01%
578 Triton X-100 in PBS) for 15 min at room temperature, and prepared for immunostaining
579 as previously described (36). Primary monoclonal or polyclonal antibodies (mAbs and
580 pAbs, respectively) antibodies against Nluc (mouse mAb; R&D Systems) for Nluc-
581 expressing viruses, GFP (goat pAb, Rockland) for Venus-expressing viruses, and anti-
582 N (mAb, 2B1) (59) were used. The Vectastain ABC kit and DAB HRP substrate kit;
583 (Vector) were used for the immunostaining following the manufacturers' specifications.
584 The plates were stained with crystal violet after the immunostaining.
585

586 **Protein gel electrophoresis and Western blot analysis**

587 Cell extracts from either mock- or virus-infected (MOI, 0.1) Vero E6 cells were
588 lysed at 24 or 48 h p.i. in radioimmunoprecipitation assay (RIPA) buffer, and proteins
589 were separated by denaturing electrophoresis. The membranes were blocked for 1 h
590 with 5% dried skim milk in TBS containing 0.1% Tween 20 (T-TBS) and incubated
591 overnight at 4°C with specific primary mAbs and pAbs: Nluc (mouse mAb; R&D
592 Systems) for Nluc-expressing viruses, GFP (goat pAb, Rockland) for Venus-
593 expressing viruses, anti-PKR (rabbit pAb, Invitrogen), NSs (pool of mAb; 5C3A1B2,
594 2A10B1B and 5F12C1B3) kindly provided by M. Groschup (45), and anti-RVFV (rabbit
595 pAb generated in the laboratory, using purified virus and detecting viral Gn/Gc and N
596 proteins) (20). A mAb against actin (Sigma) was used as an internal loading control.
597 Bound primary antibodies were detected with horseradish peroxidase (HRP)-
598 conjugated secondary antibodies against the different species (mouse, rabbit or goat).

599 Proteins were detected by chemiluminescence (Thermo Fisher Scientific) following the
600 manufacturer's recommendations and photographed using a Bio-Rad digital
601 ImageStation.
602
603 **Indirect immunofluorescence assays**
604 Vero E6 cells were mock infected or infected (MOI, 0.1) with the indicated
605 rRVFV. At 24 h p.i., the cells were fixed with 4% paraformaldehyde (PFA) and
606 permeabilized with 0.5% Triton X-100 in PBS for 15 min at room temperature and
607 blocked with PBS/5% FBS. After blocking, specific primary mAbs or pAbs for Nluc
608 (mouse mAb; R&D Systems) for Nluc-expressing viruses, GFP (goat pAb, Rockland)
609 for Venus-expressing viruses, and anti-RVFV (rabbit pAb generated in the laboratory
610 using purified virus that detects the viral Gn/Gc and N proteins) (20) were diluted in
611 blocking solution and used to separately detect protein expression using Alexa Fluor
612 594-conjugated secondary antibodies (Invitrogen). Images were taken with a Zeiss
613 Axio fluorescence microscope (Zeiss) or with a Zeiss LSM880 confocal laser
614 microscope (Zeiss).
615
616 **Flow cytometry assays**
617 Vero E6 cells were mock infected or infected (MOI, 0.01) with the indicated
618 rRVFV WT or Venus-expressing viruses. At 24 h p.i., the cells were harvested from
619 the culture, centrifuged for 2 min at 2,000 x g and incubated for 30 min at 4ºC with a
620 mAb against the N (2B1) conjugated to Alexa 700 (Invitrogen). The cells were washed
621 and fixed with fixation buffer (BioLegend) for 20 minutes at room temperature in the
622 dark. The cells were analyzed by flow cytometry by gating on green (Venus) and red

623 fluorescence (mAb anti-N 2B1 Alexa 647 conjugated) (59) using a CyFlow Cube 8
624 cytometer (Sysmex). The data were analyzed using FlowJo v10 software.
625
626 **Stability of reporter-expressing viruses in cultured cells**
627 After generation of virus working stocks (P2), confluent monolayers of Vero E6
628 cells (24-well plate format, duplicates) were infected (MOI, 0.01) with the reporter
629 expressing viruses and incubated until a 70% CPE was observed. Tissue culture
630 supernatants were then harvested and 1/10 of the collected medium was used for the
631 infection of fresh Vero E6 cells for a total of 3 passages. During each viral passage,
632 cultured supernatants were collected and plaque assays were carried out as described
633 above. Venus-expressing plaques were visualized directly using a Zeiss Axio
634 fluorescence microscope (Zeiss). To determine the stability of Nluc-expressing
635 viruses, plaques were used to infect fresh Vero E6 cells (96-well plate format, 2.5 x
636 10^4 cells/well), and Nluc activity in the tissue culture supernatants was determined at
637 48 h.p.i., as indicated above. Approximately 30 plaques per passage were evaluated
638 for each virus.
639
640 **Reporter-based microneutralization assays**
641 Nluc microneutralization assays were performed as previously described (36-
642 38). Pre- and post-challenge Sheep sera from a previous experiment carried out in the
643 laboratory were serially diluted 2-fold (starting dilution, 1/20). Then, 200 PFU of virus
644 was added to the antibody dilutions, and the mixture was incubated for 1 h at 37ºC.
645 Vero E6 cells (96-well plate format, 5 x 10^4 cells/well, triplicates) were then infected
646 with the serum-virus mixture for 1 h at 37ºC. Then, the serum-virus mixture was
647 removed and 150 µl of fresh growth medium was added and incubated for 48 h at

648 37°C. The Nluc activity in the culture supernatants was quantified using Nano-Glo
649 luciferase substrate (Promega) and a microplate reader as described previously. The
650 luciferase values of virus-infected cells in the absence of serum were used to calculate
651 100% viral infection. Cells in the absence of viral infection were used to calculate the
652 luminescence background. Triplicate wells were used to calculate the average and SD
653 of neutralization. The 50% neutralization titter (NT_{50}) was determined by use of a
654 sigmoidal dose-response curve (GraphPad Prism, v8.0.1 software).
655
656 **Antiviral assays**
657 Confluent monolayers of Vero E6 cells (96-well plate format, 5×10^4 cells/well,
658 triplicates) were infected with 200 PFU of the Nluc-reporter rRVFVs. After 1 h of
659 infection, the fresh medium was supplemented with 2-fold serial dilutions (starting
660 concentration, 1000 µM) of ribavirin (TCI), and the cells were incubated for 48 h at
661 37°C. Then, Nluc expression was quantified as indicated above. Triplicate wells were
662 used to calculate the mean and SD of inhibition. The 50% inhibitory concentration
663 (IC_{50}) was determined by use of a sigmoidal dose-response curve (GraphPad Prism,
664 v8.0.1 software).
665
666 **Mouse experiments**
667 The animals were housed under pathogen-free conditions at the biosafety level
668 3 (BSL3) animal facility of the Animal Health Research Center (CISA-INIA/CSIC),
669 Madrid (Spain). Animal experimental protocols were approved by the Ethical Review
670 Committee at the CISA-INIA/CSIC and Comunidad de Madrid (Permit number:
671 PROEX079.6/22), in strict accordance with EU guidelines 2010/63/UE about the
672 protection of animals used for experimentation and the Spanish Animal Welfare Act

673 32/2007. For pathogenicity studies, cohorts of 8-to-12-week-old BALB/C female mice
674 (N = 5/group) were intraperitoneally inoculated with the indicated viruses at the
675 indicated dose. Then, the animals were monitored daily for 18 days for clinical
676 symptoms (such as malaise, respiratory distress, and lack of movement), body weight
677 loss relative to the initial weight, and mortality. At 72 or 96 h after infection, blood
678 samples were taken by submandibular puncture and tested for viral RNA by RT-qPCR
679 (59, 79) to monitor viremia. To assess the presence of Nluc in blood samples, plasma
680 from 50 µL of the same whole blood sample was obtained, and the Nluc activity was
681 measured using a Nano-Glo Luciferase Assay Kit (Promega) and a microplate reader
682 (38). Serum samples to be used in antibody assays were collected at 18 d.p.i. (at the
683 end of the experiment) by submandibular puncture. Due to space limitations in the
684 BSL3 facility, experiments using 10^5 and $10^3/10^4$ were conducted in different
685 days/weeks. However, the same viral stocks and mouse provider were used. All the
686 inoculums were prepared via serial dilution to limit variability in the dose, and the virus
687 was back tittered after mouse inoculation to discard mistakes.
688

689 **ELISA**

690 Antibodies against N were detected by an in-house ELISA (55). Briefly, for the
691 detection of antibodies against N, sera collected at 18 d.p.i were tested (Dilution 1/100)
692 in ELISA plates adsorbed with 50 ng/well of purified recombinant N protein produced
693 from *Escherichia coli* and diluted in carbonate buffer (pH 9.6). The wells were blocked
694 with 5% BSA in PBS and 0.05% Tween 20 (PBS-T). Then, the bound antibodies were
695 detected with conjugated goat anti-mouse-IgG-HRP, and the bound conjugates were
696 detected using TMB for 10 min, followed by the addition of one volume of stopping
697 solution (3N H_2SO_4). Optical densities were measured at 450 nm (OD450).

698

699 **Statistical analysis**

700 Microsoft Excel (Microsoft Corporation) and GraphPad Prism version 10.1.2
701 (GraphPad Software, San Diego, CA, USA) software were used to analyze the data.
702 Microsoft Excel was used to perform some of the calculations and to visualize the raw
703 data. GraphPad Prism software was used to perform statistical analysis of all the data.
704 Growth kinetics were analyzed using two-way ANOVA the Dunnett's multiple
705 comparisons test. A one-way ANOVA with Tukey's method was used to evaluate viral
706 titters comparing between groups. To evaluate the Nluc activity between the different
707 groups, two-way ANOVA by Tukey's method was used. Statistical differences between
708 survival curves were analyzed using log-rank test. Viremia levels were analyzed using
709 the Dunnett's method. A P value lower than 0.05 was considered significant in all
710 cases.

711

712 **DATA AVAILABILITY STATEMENT**

713 All data supporting the findings of this study are available within the paper. No datasets
714 or new viral sequences were generated or analysed during the current study.

715

716 **ACKNOWLEDGEMENTS**

717 This study was partially funded by the Ramon y Cajal Incorporation grant (RYC-
718 2017) from the Spanish Ministry of Science, Innovation, and Universities and the
719 European Union´s Horizon Europe Research and Innovation Programme (grant
720 agreement 101046133), and by grant PID2021-122567OB-I00 funded by MCIN/ AEI
721 /10.13039/501100011033/ and by ERDF “A way of making Europe”.

722

723

724

725

726

727 **Table 1. Summary of strategies to generate reporter-expressing rRVFV.**

	Properties						
rRVFV	**Growth (Vero E6)**	**Plaque phenotype**	**Growth (C6/36)**	**Expression Nluc/Venus**	**In vitro stability**	**MN/antiviral assay**	**Virulence**
rWT	+++	+++	+++	-	ND	+++	+++
Nluc2ANSs	+++	+++	+++	++	++	+++	+
NSs2ANluc	++	+++	+++	++	+++	+++	+
Nluc2AN	++	++	++	+++	++	+++	-
N2ANluc	+	+	+	+++	+++	ND	-
Venus2ANSs	+++	+++	+++	+++	++	ND	ND
NSs2AVenus	++	++	++	+++	+++	ND	ND
Venus2AN	++	+	+	+++	+++	ND	ND

728 ND: Not determined.

729

730

731 ## REFERENCES

732 1. Mroz C, Gwida M, El-Ashker M, El-Diasty M, El-Beskawy M, Ziegler U, et al. Seroprevalence of
733 Rift Valley fever virus in livestock during inter-epidemic period in Egypt, 2014/15. BMC Vet Res.
734 2017;13(1):87.
735 2. Samy AM, Peterson AT, Hall M. Phylogeography of Rift Valley Fever Virus in Africa and the
736 Arabian Peninsula. PLoS Negl Trop Dis. 2017;11(1):e0005226.
737 3. Sang R, Arum S, Chepkorir E, Mosomtai G, Tigoi C, Sigei F, et al. Distribution and abundance of
738 key vectors of Rift Valley fever and other arboviruses in two ecologically distinct counties in Kenya.
739 PLoS Negl Trop Dis. 2017;11(2):e0005341.
740 4. Fawzy M, Helmy YA. The One Health Approach is Necessary for the Control of Rift Valley Fever
741 Infections in Egypt: A Comprehensive Review. Viruses. 2019;11(2).
742 5. Jonkmans N, D'Acremont V, Flahault A. Scoping future outbreaks: a scoping review on the
743 outbreak prediction of the WHO Blueprint list of priority diseases. BMJ Glob Health. 2021;6(9).
744 6. Grobbelaar AA, Weyer J, Leman PA, Kemp A, Paweska JT, Swanepoel R. Molecular
745 epidemiology of Rift Valley fever virus. Emerg Infect Dis. 2011;17(12):2270-6.
746 7. Terasaki K, Murakami S, Lokugamage KG, Makino S. Mechanism of tripartite RNA genome
747 packaging in Rift Valley fever virus. Proc Natl Acad Sci U S A. 2011;108(2):804-9.
748 8. Muller R, Argentini C, Bouloy M, Prehaud C, Bishop DH. Completion of the genome sequence
749 of Rift Valley fever phlebovirus indicates that the L RNA is negative sense and codes for a putative
750 transcriptase-replicase [corrected]. Nucleic Acids Res. 1991;19(19):5433.
751 9. Muller R, Poch O, Delarue M, Bishop DH, Bouloy M. Rift Valley fever virus L segment:
752 correction of the sequence and possible functional role of newly identified regions conserved in RNA-
753 dependent polymerases. J Gen Virol. 1994;75 (Pt 6):1345-52.

754 10. Huiskonen JT, Overby AK, Weber F, Grunewald K. Electron cryo-microscopy and single-particle
755 averaging of Rift Valley fever virus: evidence for GN-GC glycoprotein heterodimers. J Virol.
756 2009;83(8):3762-9.
757 11. Rusu M, Bonneau R, Holbrook MR, Watowich SJ, Birmanns S, Wriggers W, et al. An assembly
758 model of rift valley Fever virus. Front Microbiol. 2012;3:254.
759 12. Sherman MB, Freiberg AN, Holbrook MR, Watowich SJ. Single-particle cryo-electron
760 microscopy of Rift Valley fever virus. Virology. 2009;387(1):11-5.
761 13. Collett MS, Purchio AF, Keegan K, Frazier S, Hays W, Anderson DK, et al. Complete nucleotide
762 sequence of the M RNA segment of Rift Valley fever virus. Virology. 1985;144(1):228-45.
763 14. Won S, Ikegami T, Peters CJ, Makino S. NSm protein of Rift Valley fever virus suppresses virus-
764 induced apoptosis. J Virol. 2007;81(24):13335-45.
765 15. Kreher F, Tamietti C, Gommet C, Guillemot L, Ermonval M, Failloux AB, et al. The Rift Valley
766 fever accessory proteins NSm and P78/NSm-GN are distinct determinants of virus propagation in
767 vertebrate and invertebrate hosts. Emerg Microbes Infect. 2014;3(10):e71.
768 16. Giorgi C, Accardi L, Nicoletti L, Gro MC, Takehara K, Hilditch C, et al. Sequences and coding
769 strategies of the S RNAs of Toscana and Rift Valley fever viruses compared to those of Punta Toro,
770 Sicilian Sandfly fever, and Uukuniemi viruses. Virology. 1991;180(2):738-53.
771 17. Ikegami T, Won S, Peters CJ, Makino S. Characterization of Rift Valley fever virus
772 transcriptional terminations. J Virol. 2007;81(16):8421-38.
773 18. Lara E, Billecocq A, Leger P, Bouloy M. Characterization of wild-type and alternate
774 transcription termination signals in the Rift Valley fever virus genome. J Virol. 2011;85(23):12134-45.
775 19. Tercero B, Makino S. Reverse Genetics System for Rift Valley Fever Virus. Methods Mol Biol.
776 2024;2733:101-13.
777 20. Moreno S, Lorenzo G, Lopez-Valinas A, de la Losa N, Alonso C, Charro E, et al. Safety and
778 Efficacy upon Infection in Sheep with Rift Valley Fever Virus ZH548-rA2, a Triple Mutant Rescued Virus.
779 Viruses. 2024;16(1).
780 21. Calvo-Pinilla E, Marin-Lopez A, Moreno S, Lorenzo G, Utrilla-Trigo S, Jimenez-Cabello L, et al.
781 A protective bivalent vaccine against Rift Valley fever and bluetongue. NPJ Vaccines. 2020;5(1):70.
782 22. Billecocq A, Gauliard N, Le May N, Elliott RM, Flick R, Bouloy M. RNA polymerase I-mediated
783 expression of viral RNA for the rescue of infectious virulent and avirulent Rift Valley fever viruses.
784 Virology. 2008;378(2):377-84.
785 23. Bouloy M, Flick R. Reverse genetics technology for Rift Valley fever virus: current and future
786 applications for the development of therapeutics and vaccines. Antiviral Res. 2009;84(2):101-18.
787 24. Habjan M, Penski N, Spiegel M, Weber F. T7 RNA polymerase-dependent and -independent
788 systems for cDNA-based rescue of Rift Valley fever virus. J Gen Virol. 2008;89(Pt 9):2157-66.
789 25. Ikegami T. Development of a Simian RNA Polymerase I Promoter-Driven Reverse Genetics for
790 the Rescue of Recombinant Rift Valley Fever Virus from Vero Cells. J Virol. 2021;95(7).
791 26. Ikegami T, Won S, Peters CJ, Makino S. Rescue of infectious rift valley fever virus entirely from
792 cDNA, analysis of virus lacking the NSs gene, and expression of a foreign gene. J Virol. 2006;80(6):2933-
793 40.
794 27. Murakami S, Terasaki K, Makino S. Generation of a Single-Cycle Replicable Rift Valley Fever
795 Vaccine. Methods Mol Biol. 2016;1403:187-206.
796 28. Terasaki K, Kalveram B, Johnson KN, Juelich T, Smith JK, Zhang L, et al. Rift Valley fever virus
797 78kDa envelope protein attenuates virus replication in macrophage-derived cell lines and viral
798 virulence in mice. PLoS Negl Trop Dis. 2021;15(9):e0009785.
799 29. Wichgers Schreur PJ, Oreshkova N, Moormann RJ, Kortekaas J. Creation of Rift Valley fever
800 viruses with four-segmented genomes reveals flexibility in bunyavirus genome packaging. J Virol.
801 2014;88(18):10883-93.
802 30. Hall MP, Unch J, Binkowski BF, Valley MP, Butler BL, Wood MG, et al. Engineered luciferase
803 reporter from a deep sea shrimp utilizing a novel imidazopyrazinone substrate. ACS Chem Biol.
804 2012;7(11):1848-57.

805 31. Shaner NC, Patterson GH, Davidson MW. Advances in fluorescent protein technology. J Cell
806 Sci. 2007;120(Pt 24):4247-60.
807 32. Shaner NC, Steinbach PA, Tsien RY. A guide to choosing fluorescent proteins. Nat Methods.
808 2005;2(12):905-9.
809 33. Welsh DK, Noguchi T. Cellular bioluminescence imaging. Cold Spring Harb Protoc.
810 2012;2012(8).
811 34. Zhao H, Doyle TC, Coquoz O, Kalish F, Rice BW, Contag CH. Emission spectra of bioluminescent
812 reporters and interaction with mammalian tissue determine the sensitivity of detection in vivo. J
813 Biomed Opt. 2005;10(4):41210.
814 35. Stacer AC, Nyati S, Moudgil P, Iyengar R, Luker KE, Rehemtulla A, et al. NanoLuc reporter for
815 dual luciferase imaging in living animals. Mol Imaging. 2013;12(7):1-13.
816 36. Nogales A, Avila-Perez G, Rangel-Moreno J, Chiem K, DeDiego ML, Martinez-Sobrido L. A Novel
817 Fluorescent and Bioluminescent Bireporter Influenza A Virus To Evaluate Viral Infections. J Virol.
818 2019;93(10).
819 37. Chiem K, Nogales A, Lorenzo M, Morales Vasquez D, Xiang Y, Gupta YK, et al. Identification of
820 In Vitro Inhibitors of Monkeypox Replication. Microbiol Spectr. 2023;11(4):e0474522.
821 38. Utrilla-Trigo S, Jimenez-Cabello L, Marin-Lopez A, Illescas-Amo M, Andres G, Calvo-Pinilla E, et
822 al. Engineering recombinant replication-competent bluetongue viruses expressing reporter genes for
823 in vitro and non-invasive in vivo studies. Microbiol Spectr. 2024;12(3):e0249323.
824 39. Chiem K, Park JG, Morales Vasquez D, Plemper RK, Torrelles JB, Kobie JJ, et al. Monitoring
825 SARS-CoV-2 Infection Using a Double Reporter-Expressing Virus. Microbiol Spectr.
826 2022;10(5):e0237922.
827 40. Brennan B, Welch SR, Elliott RM. The consequences of reconfiguring the ambisense S genome
828 segment of Rift Valley fever virus on viral replication in mammalian and mosquito cells and for genome
829 packaging. PLoS Pathog. 2014;10(2):e1003922.
830 41. Breen M, Nogales A, Baker SF, Martinez-Sobrido L. Replication-Competent Influenza A Viruses
831 Expressing Reporter Genes. Viruses. 2016;8(7).
832 42. DiPiazza A, Nogales A, Poulton N, Wilson PC, Martinez-Sobrido L, Sant AJ. Pandemic 2009
833 H1N1 Influenza Venus reporter virus reveals broad diversity of MHC class II-positive antigen-bearing
834 cells following infection in vivo. Sci Rep. 2017;7(1):10857.
835 43. Kim JH, Lee SR, Li LH, Park HJ, Park JH, Lee KY, et al. High cleavage efficiency of a 2A peptide
836 derived from porcine teschovirus-1 in human cell lines, zebrafish and mice. PLoS One.
837 2011;6(4):e18556.
838 44. Liu Z, Chen O, Wall JBJ, Zheng M, Zhou Y, Wang L, et al. Systematic comparison of 2A peptides
839 for cloning multi-genes in a polycistronic vector. Sci Rep. 2017;7(1):2193.
840 45. Borrego B, Moreno S, de la Losa N, Weber F, Brun A. The Change P82L in the Rift Valley Fever
841 Virus NSs Protein Confers Attenuation in Mice. Viruses. 2021;13(4).
842 46. Habjan M, Pichlmair A, Elliott RM, Overby AK, Glatter T, Gstaiger M, et al. NSs protein of rift
843 valley fever virus induces the specific degradation of the double-stranded RNA-dependent protein
844 kinase. J Virol. 2009;83(9):4365-75.
845 47. Ikegami T, Narayanan K, Won S, Kamitani W, Peters CJ, Makino S. Rift Valley fever virus NSs
846 protein promotes post-transcriptional downregulation of protein kinase PKR and inhibits eIF2alpha
847 phosphorylation. PLoS Pathog. 2009;5(2):e1000287.
848 48. Atkins C, Freiberg AN. Recent advances in the development of antiviral therapeutics for Rift
849 Valley fever virus infection. Future Virol. 2017;12(11):651-65.
850 49. Kende M, Lupton HW, Rill WL, Levy HB, Canonico PG. Enhanced therapeutic efficacy of
851 poly(ICLC) and ribavirin combinations against Rift Valley fever virus infection in mice. Antimicrob
852 Agents Chemother. 1987;31(7):986-90.
853 50. Lang Y, Li Y, Jasperson D, Henningson J, Lee J, Ma J, et al. Identification and evaluation of
854 antivirals for Rift Valley fever virus. Vet Microbiol. 2019;230:110-6.

855 51. Scharton D, Bailey KW, Vest Z, Westover JB, Kumaki Y, Van Wettere A, et al. Favipiravir (T-705)
856 protects against peracute Rift Valley fever virus infection and reduces delayed-onset neurologic
857 disease observed with ribavirin treatment. Antiviral Res. 2014;104:84-92.
858 52. Geerling E, Murphy V, Mai MC, Stone ET, Casals AG, Hassert M, et al. Metal coordinating
859 inhibitors of Rift Valley fever virus replication. PLoS One. 2022;17(9):e0274266.
860 53. Cartwright HN, Barbeau DJ, Doyle JD, Klein E, Heise MT, Ferris MT, et al. Genetic diversity of
861 collaborative cross mice enables identification of novel rift valley fever virus encephalitis model. PLoS
862 Pathog. 2022;18(7):e1010649.
863 54. Ikegami T, Jurado-Cobena E, Alkan C, Smith JK, Zhang L, Kalveram B, et al. Evaluations of
864 rationally designed rift valley fever vaccine candidate RVax-1 in mosquito and rodent models. NPJ
865 Vaccines. 2022;7(1):109.
866 55. Borrego B, Brun A. A Hyper-Attenuated Variant of Rift Valley Fever Virus Generated by a
867 Mutagenic Drug (Favipiravir) Unveils Potential Virulence Markers. Front Microbiol. 2020;11:621463.
868 56. Borrego B, Moreno S, Lopez-Valinas A, de la Losa N, Weber F, Nunez JI, et al. Identification of
869 Single Amino Acid Changes in the Rift Valley Fever Virus Polymerase Core Domain Contributing to Virus
870 Attenuation In Vivo. Front Cell Infect Microbiol. 2022;12:875539.
871 57. Crespo Leon F, Gutierrez Diez F, Rodriguez Ferri F, Leon Vizcaino L, Cuello Gijon F, Gimeno EJ,
872 et al. The translation into Spanish of the OIE Manual of diagnostic tests and vaccines for terrestrial
873 animals (mammals, birds and bees): problems, solutions and conclusions. Rev Sci Tech.
874 2005;24(3):1095-104.
875 58. Cullinane AA, Garvey M. A review of diagnostic tests recommended by the World Organisation
876 for Animal Health. Rev Sci Tech Oie. 2021;40(1):75-89.
877 59. Moreno S, Calvo-Pinilla E, Devignot S, Weber F, Ortego J, Brun A. Recombinant Rift Valley fever
878 viruses encoding bluetongue virus (BTV) antigens: Immunity and efficacy studies upon a BTV-4
879 challenge. PLoS Negl Trop Dis. 2020;14(12):e0008942.
880 60. Tran V, Moser LA, Poole DS, Mehle A. Highly sensitive real-time in vivo imaging of an influenza
881 reporter virus reveals dynamics of replication and spread. J Virol. 2013;87(24):13321-9.
882 61. Cartwright HN, Barbeau DJ, McElroy AK. Rift Valley Fever Virus Is Lethal in Different Inbred
883 Mouse Strains Independent of Sex. Front Microbiol. 2020;11:1962.
884 62. Lathan R, Simon-Chazottes D, Jouvion G, Godon O, Malissen M, Flamand M, et al. Innate
885 Immune Basis for Rift Valley Fever Susceptibility in Mouse Models. Sci Rep. 2017;7(1):7096.
886 63. Graham VA, Easterbrook L, Kennedy E, Rayner E, Findlay-Wilson S, Flett L, et al. Pathogenesis
887 of Rift Valley Fever Virus in a BALB/c Mouse Model Is Affected by Virus Culture Conditions and Sex of
888 the Animals. Viruses. 2023;15(12).
889 64. Tokuda S, Do Valle TZ, Batista L, Simon-Chazottes D, Guillemot L, Bouloy M, et al. The genetic
890 basis for susceptibility to Rift Valley fever disease in MBT/Pas mice. Genes Immun. 2015;16(3):206-12.
891 65. Kohl A, di Bartolo V, Bouloy M. The Rift Valley fever virus nonstructural protein NSs is
892 phosphorylated at serine residues located in casein kinase II consensus motifs in the carboxy-terminus.
893 Virology. 1999;263(2):517-25.
894 66. Le May N, Mansuroglu Z, Leger P, Josse T, Blot G, Billecocq A, et al. A SAP30 complex inhibits
895 IFN-beta expression in Rift Valley fever virus infected cells. PLoS Pathog. 2008;4(1):e13.
896 67. Billecocq A, Spiegel M, Vialat P, Kohl A, Weber F, Bouloy M, et al. NSs protein of Rift Valley
897 fever virus blocks interferon production by inhibiting host gene transcription. J Virol.
898 2004;78(18):9798-806.
899 68. Li S, Zhu X, Guan Z, Huang W, Zhang Y, Kortekaas J, et al. NSs Filament Formation Is Important
900 but Not Sufficient for RVFV Virulence In Vivo. Viruses. 2019;11(9).
901 69. Hayashi M, Schultz EP, Lanchy JM, Lodmell JS. Time-Resolved Analysis of N-RNA Interactions
902 during RVFV Infection Shows Qualitative and Quantitative Shifts in RNA Encapsidation and Packaging.
903 Viruses. 2021;13(12).

904 70. Overby AK, Popov VL, Pettersson RF, Neve EP. The cytoplasmic tails of Uukuniemi Virus
905 (Bunyaviridae) G(N) and G(C) glycoproteins are important for intracellular targeting and the budding
906 of virus-like particles. J Virol. 2007;81(20):11381-91.
907 71. Ferron F, Li Z, Danek EI, Luo D, Wong Y, Coutard B, et al. The hexamer structure of Rift Valley
908 fever virus nucleoprotein suggests a mechanism for its assembly into ribonucleoprotein complexes.
909 PLoS Pathog. 2011;7(5):e1002030.
910 72. Raymond DD, Piper ME, Gerrard SR, Skiniotis G, Smith JL. Phleboviruses encapsidate their
911 genomes by sequestering RNA bases. Proc Natl Acad Sci U S A. 2012;109(47):19208-13.
912 73. Raymond DD, Piper ME, Gerrard SR, Smith JL. Structure of the Rift Valley fever virus
913 nucleocapsid protein reveals another architecture for RNA encapsidation. Proc Natl Acad Sci U S A.
914 2010;107(26):11769-74.
915 74. Murakami S, Terasaki K, Narayanan K, Makino S. Roles of the coding and noncoding regions of
916 rift valley Fever virus RNA genome segments in viral RNA packaging. J Virol. 2012;86(7):4034-9.
917 75. Piper ME, Sorenson DR, Gerrard SR. Efficient cellular release of Rift Valley fever virus requires
918 genomic RNA. PLoS One. 2011;6(3):e18070.
919 76. Tercero B, Terasaki K, Narayanan K, Makino S. Mechanistic insight into the efficient packaging
920 of antigenomic S RNA into Rift Valley fever virus particles. Front Cell Infect Microbiol.
921 2023;13:1132757.
922 77. Buchholz UJ, Finke S, Conzelmann KK. Generation of bovine respiratory syncytial virus (BRSV)
923 from cDNA: BRSV NS2 is not essential for virus replication in tissue culture, and the human RSV leader
924 region acts as a functional BRSV genome promoter. J Virol. 1999;73(1):251-9.
925 78. Borrego B, de Avila AI, Domingo E, Brun A. Lethal Mutagenesis of Rift Valley Fever Virus
926 Induced by Favipiravir. Antimicrob Agents Chemother. 2019;63(8).
927 79. Mwaengo D, Lorenzo G, Iglesias J, Warigia M, Sang R, Bishop RP, et al. Detection and
928 identification of Rift Valley fever virus in mosquito vectors by quantitative real-time PCR. Virus Res.
929 2012;169(1):137-43.

930

931 **FIGURES**

932 **Figure 1. Schematic representation of the RVFV segment S.** RVFV segment S and
933 its viral products are indicated by blue (N) or gray (NSs) boxes. The black and striped
934 red boxes denote untranslated regions and intergenic regions, respectively. The
935 sequences of the reporter and 2A are indicated in green and red boxes, respectively.

936

937 **Figure 2. Multicycle growth kinetics.** Vero E6 cells (12-well plates, triplicates) were
938 infected (MOI of 0.01) with rRVFV WT (rWT) or with recombinant viruses expressing
939 Nluc (**A and B**) or Venus (**C and D**). At the indicated h.p.i. (24, 48 and 72), viral titers
940 in culture supernatants were evaluated by plaque assay (PFU/ml), and the same rWT
941 representation was used in A and D (A and D). Comparison of the replication curves

942 of viruses expressing Nluc or Venus versus rWT at different post-infection times
943 revealed statistically significant differences (Dunnett's method). * P < 0.05; ** P <
944 0.0021; *** P < 0.0002; **** P < 0.0001. The data represent the means ± SDs of
945 triplicate samples. At the same time, post-infection Nluc activity was evaluated (RLU:
946 Relative Light Units) (**B**), and Venus expression was analyzed using a fluorescence
947 microscope (**C**). Representative images are shown. Scale bars, 100 µm. Dotted line
948 indicates the limit of detection (100 FFU/ml) of the assay.
949
950 **Figure 3. Plaque assays.** Vero E6 cells (10^6 cells/well, 6-well plate format) were
951 infected with rRVFV WT (rWT) or with recombinant viruses expressing Venus (top) or
952 Nluc (bottom) and incubated at 37ºC for 3 days. Plaques were evaluated by
953 immunostaining with the mAb anti-N (2B1), the goat pAb anti-GFP (top) or the mAb
954 anti-Nluc (bottom). Immunostaining of rWT was performed with the mAb anti-N (2B1)
955 or a combination of the goat pAb anti-GFP and the mAb anti-Nluc.
956
957 **Figure 4. Analysis of protein expression by IFA.** Vero E6 cells were infected with
958 the indicated virus at an MOI of 0.1 or mock infected. At 24 h p.i., the cells were fixed
959 and permeabilized. Protein expression was examined by IFA using a rabbit pAb
960 against RVFV or mAb for Nluc (**A**) or a goat pAb against GFP (**B**). Scale bars, 100 µm.
961 (**C**) **Confocal microscopy of Nluc-expressing rRVFV.** Protein expression was
962 examined by confocal microscopy using the indicated antibodies. Arrows shows the
963 presence characteristic intranuclear NSs filaments (Nluc2ANSs and NSs2ANluc) and
964 colocalization of Nluc with viral proteins (Nluc2AN and N2ANluc).
965

966 **Figure 5. Analysis of protein expression by WB.** Vero E6 cells were infected with
967 Nluc- (**A**) or Venus-expressing (**B**) rRVFV at an MOI of 0.01 or mock infected. At 24
968 or 48 h p.i, cell extracts were prepared in RIPA buffer. Protein expression was
969 examined by Western blotting using specific antibodies for viral proteins: pAb against
970 RVFV for N and Gn, a pool of mAbs against NSs (after stripping of pAb). In addition,
971 the expression of the reporter genes Nluc (**A**) and Venus (**B**) was evaluated. Actin was
972 used as a loading control. The numbers on the left indicate the molecular size of the
973 protein markers (in kilodaltons). (**C** and **D**) **Degradation of PKR in rRVFV infected**
974 **cells.** HEK293T cells were infected at a MOI of 0.1 with the indicated viruses. Cells
975 were harvested at 24 hpi and analyzed by Western blot using a pAb anti-PKR, a pAb
976 against RVFV for N and Gn/Gc, and an anti-actin antibody as primary antibodies.
977
978 **Figure 6. Nluc activity in tissue culture supernatant *versus* cell extracts and**
979 **Venus expression by Flow cytometry analysis.** Vero E6 cells (24-well plates,
980 triplicates) were infected (MOI of 0.01) with recombinant viruses expressing Nluc. At
981 48 h p.i., viral titers in culture supernatants were evaluated by plaque assay (PFU/ml).
982 The differences between the groups were calculated using one-way ANOVA with the
983 Tukey method. * $P < 0.05$; *** $P < 0.0002$; **** $P < 0.0001$ (**A**). Nluc activity in tissue
984 culture supernatants (TCSs) and cell extracts was measured. RLU: Relative Light
985 Units. The differences between the groups were calculated using two-way ANOVA
986 with the Tukey method. * $P < 0.05$; *** $P < 0.0002$; **** $P < 0.0001$. (**B**). The data
987 represent the means ± SDs of triplicate samples. (**C**) Flow cytometry analysis. Vero
988 E6 cells were infected (MOI of 0.01) with recombinant viruses expressing Venus. At
989 24 h p.i., the cells were harvested from the culture and stained with a mAb against N
990 conjugated with Alexa 700. The cells were analyzed by flow cytometry by gating on

991 green (Venus) and red fluorescence (mAb anti-N 2B1) and the percentage of N+,
992 Venus+ or Venus+/N+ is indicated.
993
994 **Figure 7. Genetic stability of reporter-expressing RVFVs in vitro.** (**A**) After the
995 generation of virus working stocks (P2), the recombinant viruses were passaged up to
996 3 times in Vero E6 cells (P3 to P5). Stability is expressed as the percentage of plaques
997 that expressed Nluc (**B**) or Venus (**C**) reporter genes in each passage.
998
999 **Figure 8. A luciferase-based microneutralization assay for assessing RVFV**
1000 **antivirals and neutralizing antibodies.** (**A and B**) **Antiviral.** Vero E6 cells (96-well
1001 plates, 2 x 10^4 cells/well, triplicates) were infected with 200 PFU of Nluc-expressing
1002 rRVFV and incubated with 2-fold serial dilutions (starting concentration, 1000 μM) of
1003 ribavirin. Inhibition of viral replication was evaluated by quantifying Nluc reporter
1004 expression at 48 h p.i. The differences between the groups were calculated using two-
1005 way ANOVA with the Tukey method. * $P < 0.05$; *** $P < 0.0002$; **** $P < 0.0001$. (**A**).
1006 The percent inhibition (IC_{50}) was calculated using sigmoidal dose-response curves
1007 (**B**). As an internal control, infected cells were not treated with antivirals. The
1008 percentage of viral inhibition was normalized to that with infection in the absence of
1009 antivirals. The data are presented as the means ± SDs of the results determined in
1010 triplicate. (**C and D**) **Neutralizing antibodies.** Two hundred PFU of Nluc-expressing
1011 rRVFV were pre-incubated with 2-fold serial dilutions (starting dilution, 1:20) of sheep
1012 sera collected before or after vaccination for 1 h. Subsequently, Vero E6 cells (96-well
1013 plates, 2 x 10^4 cells/well, triplicates) were infected with the sera-virus mixture. (**A**) Virus
1014 neutralization was determined by quantitating Nluc reporter expression at 48 h p.i. (**B**)
1015 The percent neutralization (NT_{50}) was calculated using sigmoidal dose-response

1016 curves. Infected cells in the absence of serum and mock-infected cells were used as
1017 internal controls. The data are presented as the means ± SDs of the results determined
1018 in triplicate.
1019
1020 **Figure 9. Multicycle growth kinetics in insect cells.** C6/36 mosquito cells (T25
1021 flasks, triplicates) were infected (MOI of 0.01) with rRVFV WT (rWT) or with
1022 recombinant viruses expressing Nluc (**A and B**) or Venus (**C and D**). At the indicated
1023 days p.i. (3, 5, and 7), viral titers in culture supernatants were evaluated by plaque
1024 assay (PFU/ml), and the same rWT representation was used in A and C. Dunnett's
1025 method was used to statistically compare viruses expressing Nluc or Venus versus
1026 rWT. * $P < 0.05$; ** $P < 0.0021$; *** $P < 0.0002$; **** $P < 0.0001$ (**A and C**). The data
1027 represent the means ± SDs of triplicate samples. At the same time, p.i. Nluc activity
1028 (RLU: Relative Light Units) was measured in (**B**), and Venus expression was
1029 evaluated using a fluorescence microscope (**D**). Representative images are shown.
1030 Scale bars, 100 µm. Dotted line indicates the limit of detection (100 FFU/ml) of the
1031 assay.
1032
1033 **Figure 10. In vivo virulence of Nluc-expressing rRVFV.** Groups of 8-to-12-week-
1034 old BALB/C female mice (N= 5/group) were infected with 10^3, 10^4 or 10^5 PFU/mouse
1035 of the indicated viruses: rWT or the Nluc-expressing viruses. Weight loss (**A**) and
1036 survival (**B**) were evaluated daily for 18 days. The statistical differences between the
1037 curves of recombinant viruses expressing NLuc versus rWT were calculated using the
1038 log-rank test, with a P-value < 0.05. (**C**) Viremia determined by RT-qPCR in EDTA-
1039 treated blood samples collected at day 3 and 5 p.i. Cutoff: Cq ≥ 37 (dotted grey line).
1040 Points represent individual Cq value for each mouse, and lines of the corresponding

1041 colour represent the mean Cq value of each group. Dunnett's method was used to
1042 statistically compare viruses expressing Nluc versus rWT. * $P < 0.05$; ** $P < 0.0021$;
1043 *** $P < 0.0002$; **** $P < 0.0001$. (**D**) Antibody responses in surviving mice were
1044 evaluated by ELISA (using purified N protein) on day 18 p.i., to confirm
1045 seroconversion. Mouse sera were diluted 1:100.
1046

Figure 1

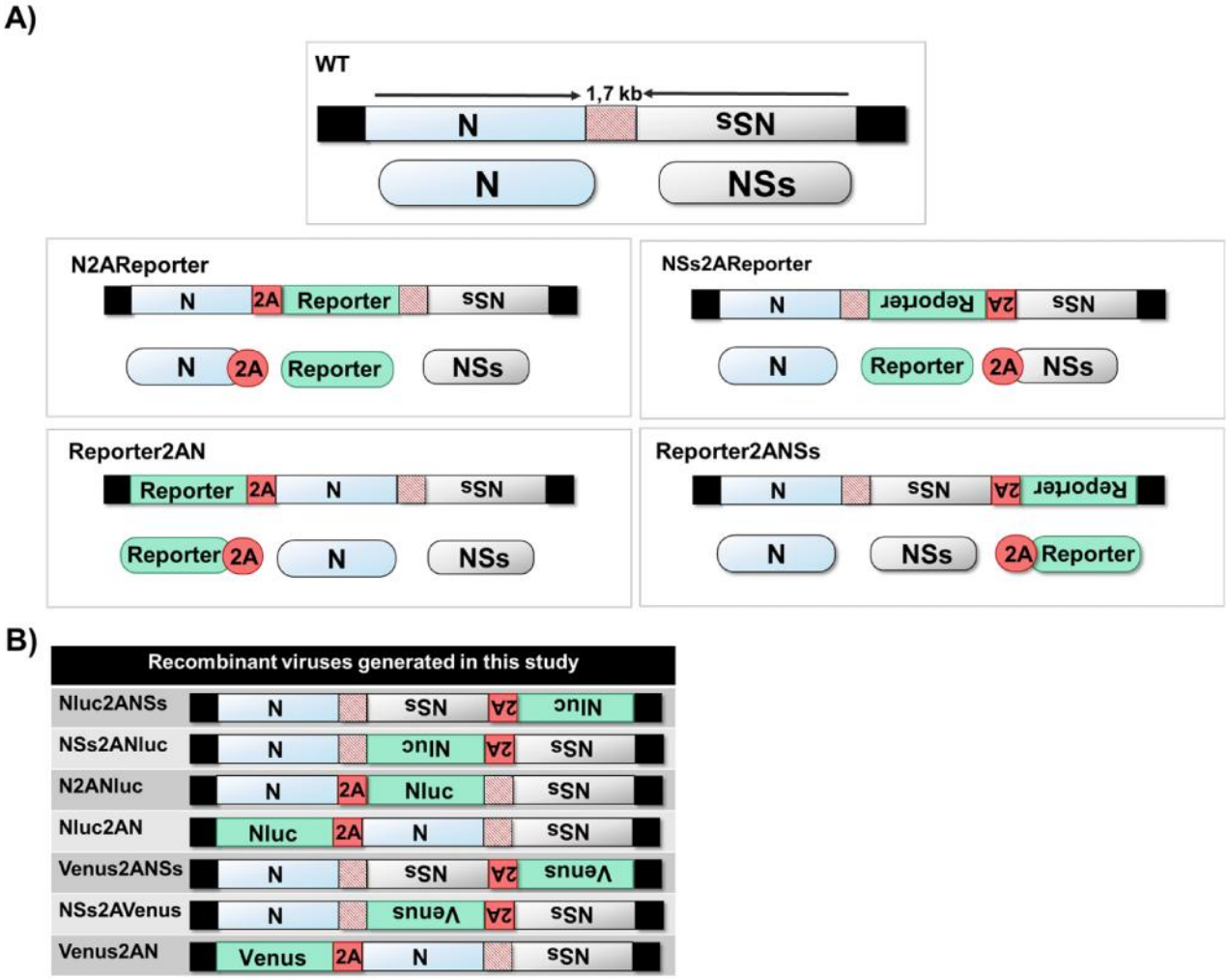
A)
WT
1,7 kb
N
NSs
N2AReporter
2A
Reporter
NSs2AReporter
Reporter2AN
Reporter2ANSs
B)
Recombinant viruses generated in this study
Nluc2ANSs
NSs2ANluc
N2ANluc
Nluc2AN
Venus2ANSs
NSs2AVenus
Venus2AN
Nluc
Venus

Figure 2

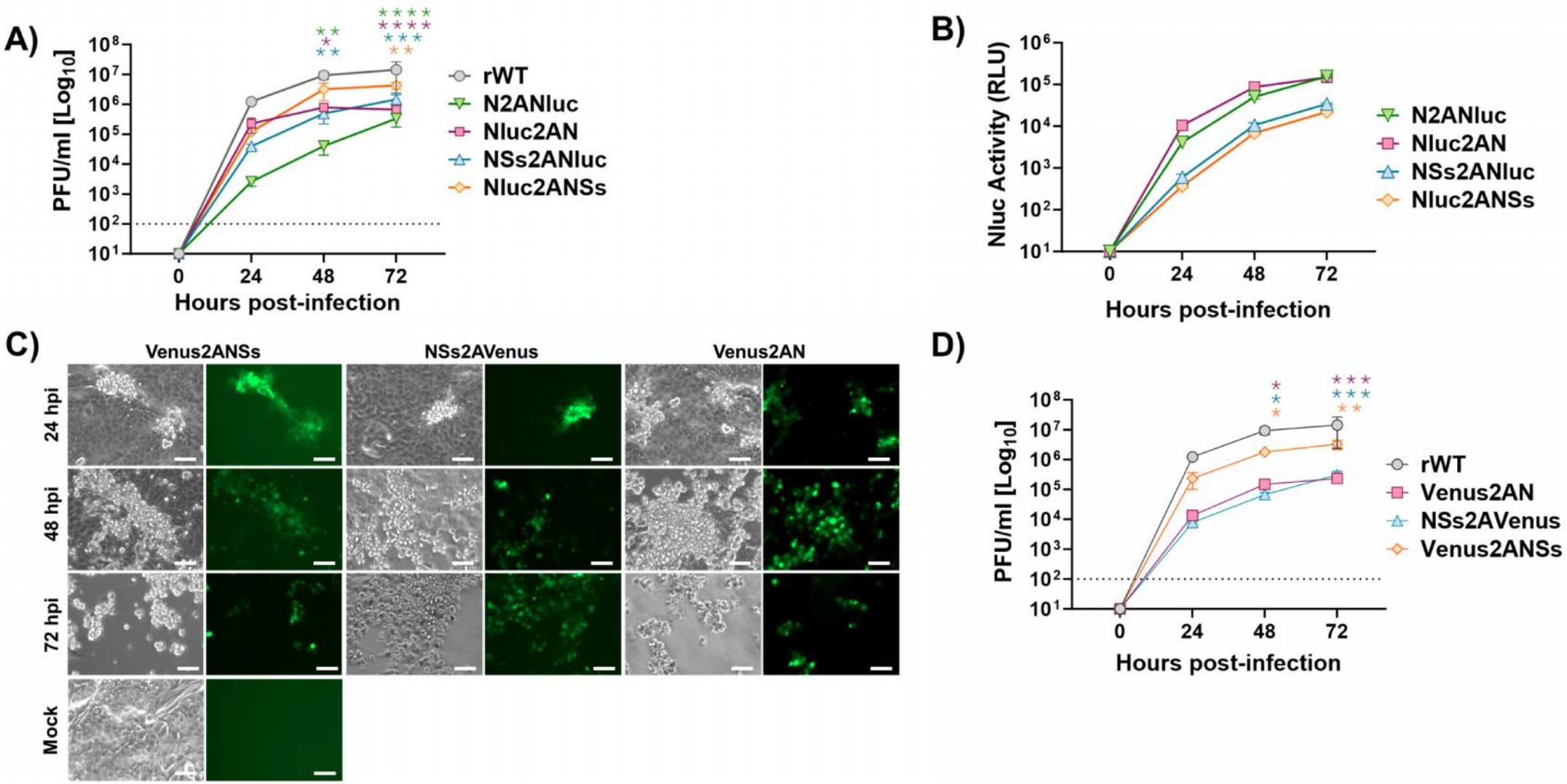
A)
PFU/ml [Log10]
Hours post-infection
rWT
N2ANluc
Nluc2AN
NSs2ANluc
Nluc2ANSs
B)
Nluc Activity (RLU)
Hours post-infection
N2ANluc
Nluc2AN
NSs2ANluc
Nluc2ANSs
C)
Venus2ANSs
NSs2AVenus
Venus2AN
24 hpi
48 hpi
72 hpi
Mock
D)
PFU/ml [Log10]
Hours post-infection
rWT
Venus2AN
NSs2AVenus
Venus2ANSs

Figure 3

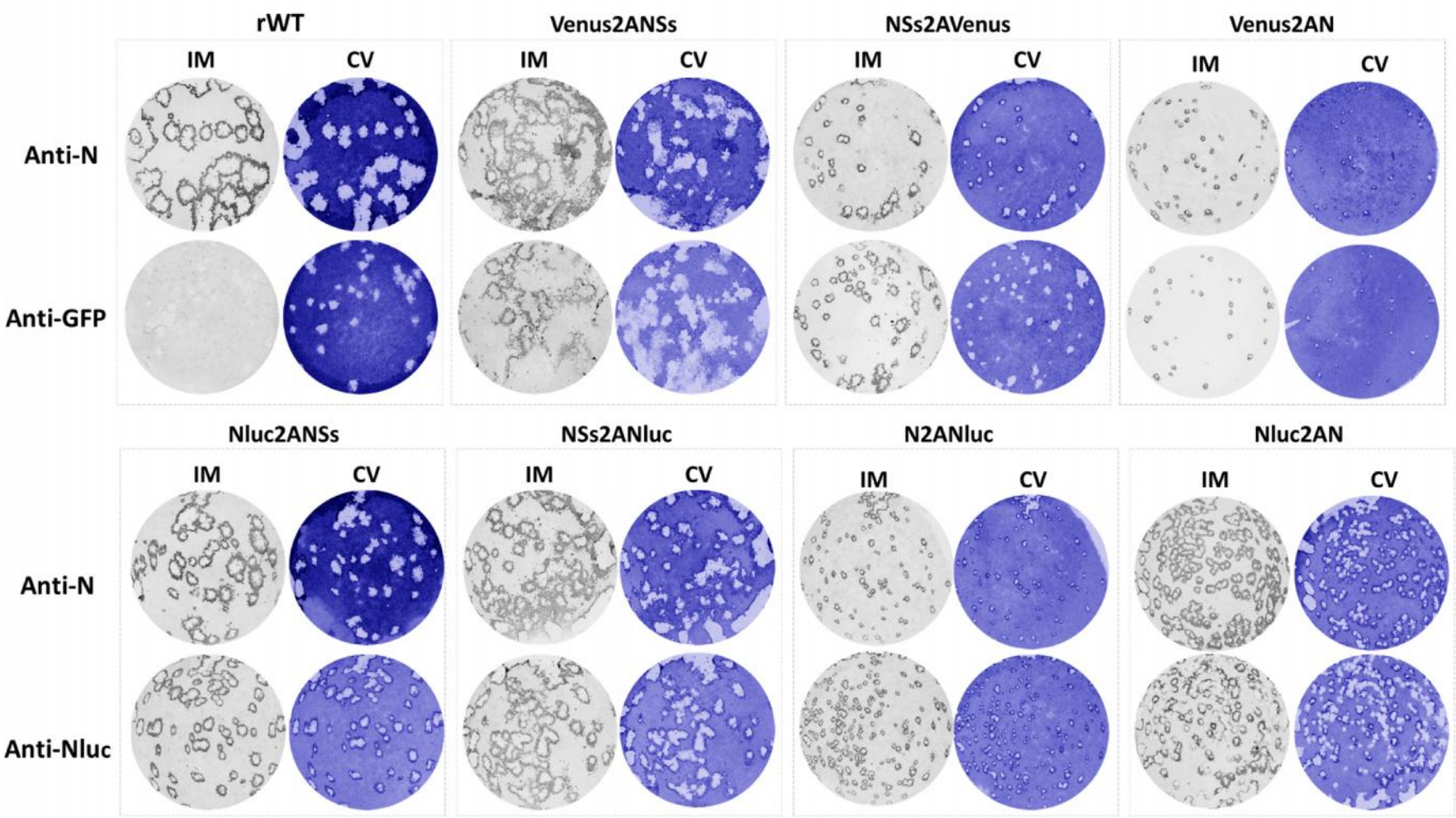
rWT
Venus2ANSs
NSs2AVenus
Venus2AN
IM
CV
Anti-N
Anti-GFP
Nluc2ANSs
NSs2ANluc
N2ANluc
Nluc2AN
Anti-Nluc

Figure 4

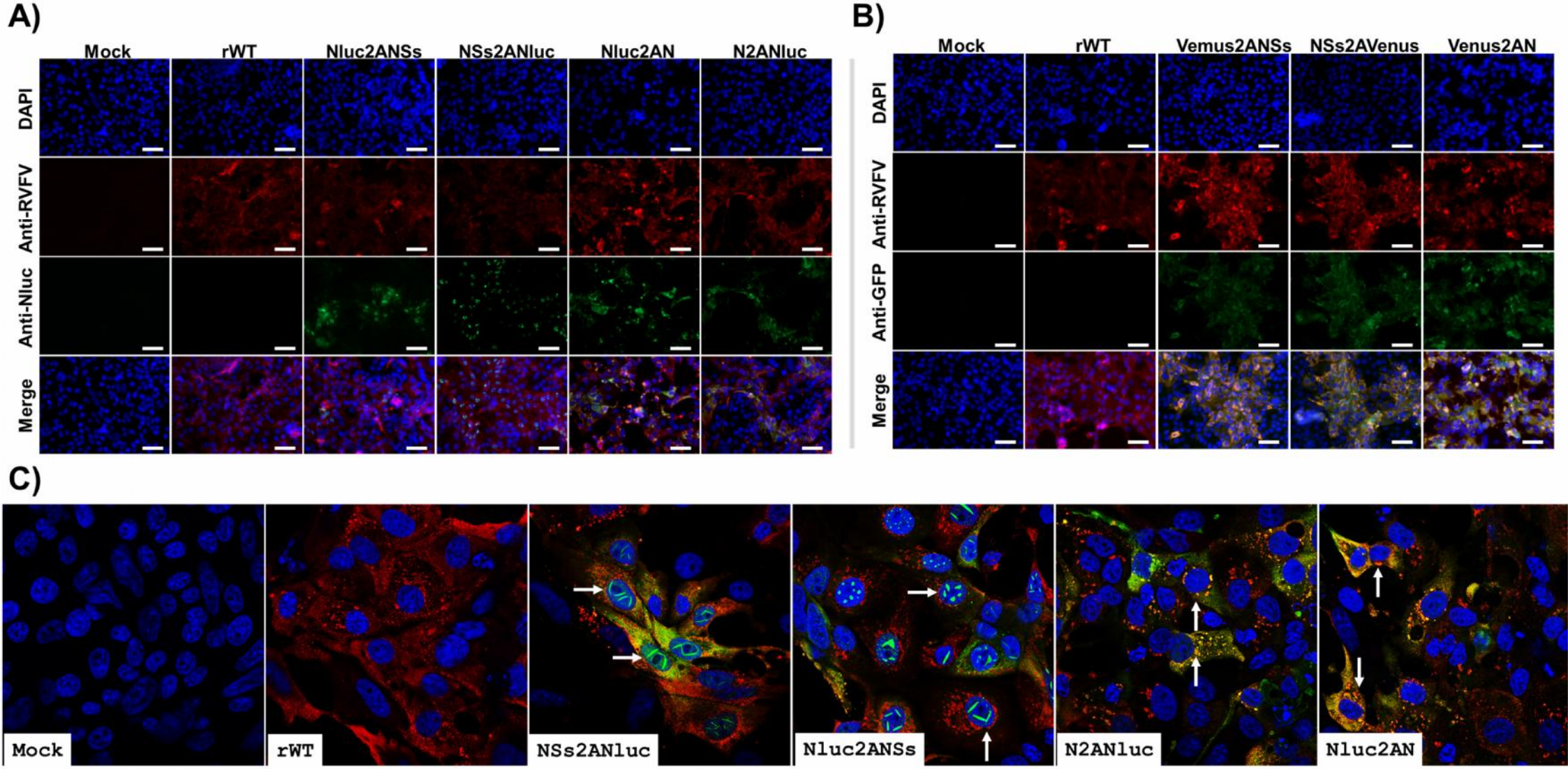
A)
Mock
rWT
Nluc2ANSs
NSs2ANluc
Nluc2AN
N2ANluc
DAPI
Anti-RVFV
Anti-Nluc
Merge
B)
Mock
rWT
Vemus2ANSs
NSs2AVenus
Venus2AN
DAPI
Anti-RVFV
Anti-GFP
Merge
C)
Mock
rWT
NSs2ANluc
Nluc2ANSs
N2ANluc
Nluc2AN

Figure 5

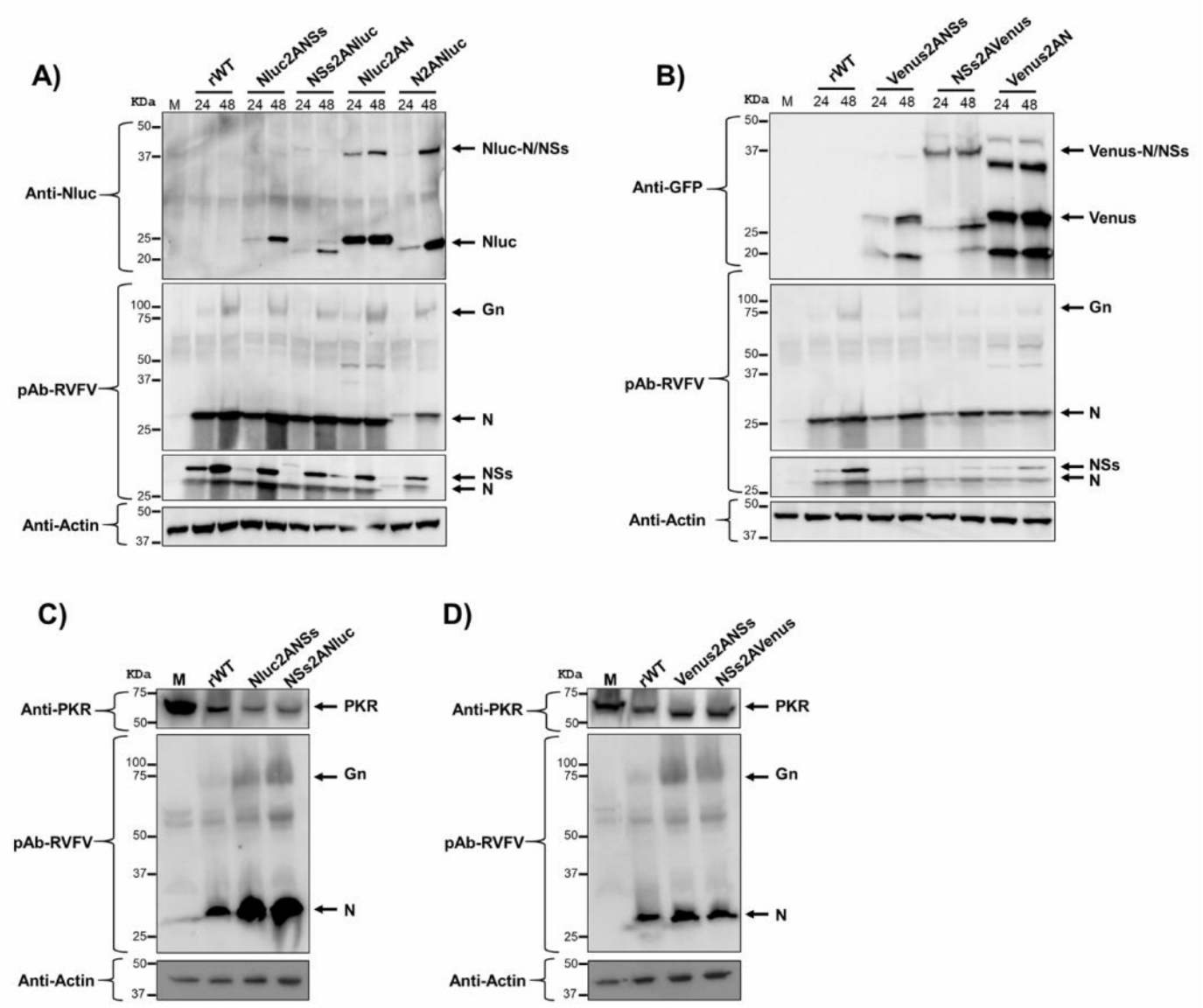
A)
rWT
Nluc2ANSs
NSs2ANluc
Nluc2AN
N2ANluc
KDa
M
24 48 24 48 24 48 24 48 24 48
Anti-Nluc
Nluc-N/NSs
Nluc
pAb-RVFV
Gn
N
NSs
N
Anti-Actin
B)
rWT
Venus2ANSs
NSs2AVenus
Venus2AN
Anti-GFP
Venus-N/NSs
Venus
pAb-RVFV
Gn
N
NSs
N
Anti-Actin
C)
M
rWT
Nluc2ANSs
NSs2ANluc
Anti-PKR
PKR
pAb-RVFV
Gn
N
Anti-Actin
D)
M
rWT
Venus2ANSs
NSs2AVenus
Anti-PKR
PKR
pAb-RVFV
Gn
N
Anti-Actin

Figure 6

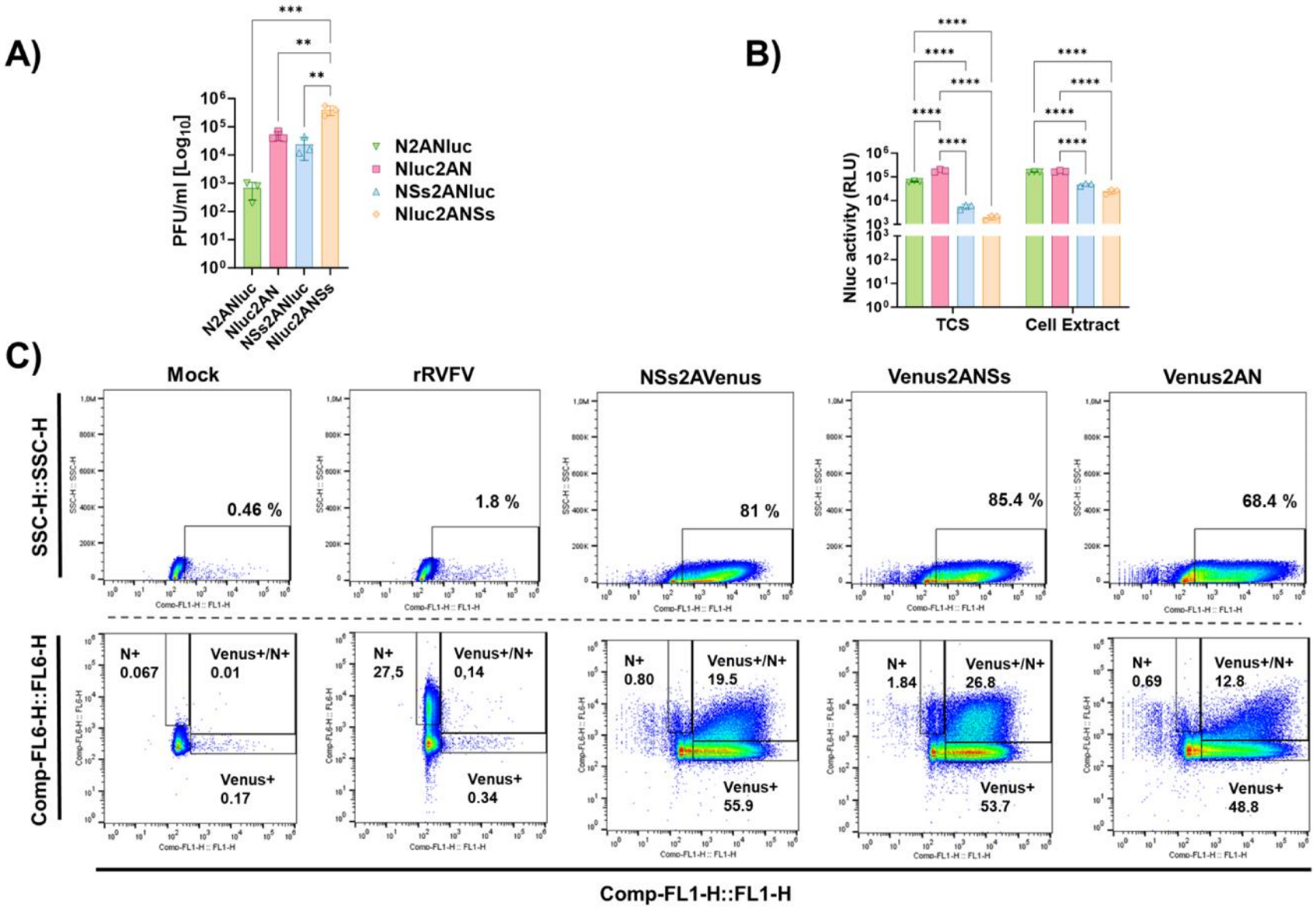
A)
PFU/ml [Log10]
N2ANluc
Nluc2AN
NSs2ANluc
Nluc2ANSs
B)
Nluc activity (RLU)
TCS
Cell Extract
C)
Mock
rRVFV
NSs2AVenus
Venus2ANSs
Venus2AN
SSC-H::SSC-H
Comp-FL6-H::FL6-H
Comp-FL1-H::FL1-H
0.46 %
1.8 %
81 %
85.4 %
68.4 %
N+ 0.067
Venus+/N+ 0.01
Venus+ 0.17
N+ 27,5
Venus+/N+ 0,14
Venus+ 0.34
N+ 0.80
Venus+/N+ 19.5
Venus+ 55.9
N+ 1.84
Venus+/N+ 26.8
Venus+ 53.7
N+ 0.69
Venus+/N+ 12.8
Venus+ 48.8

Figure 7

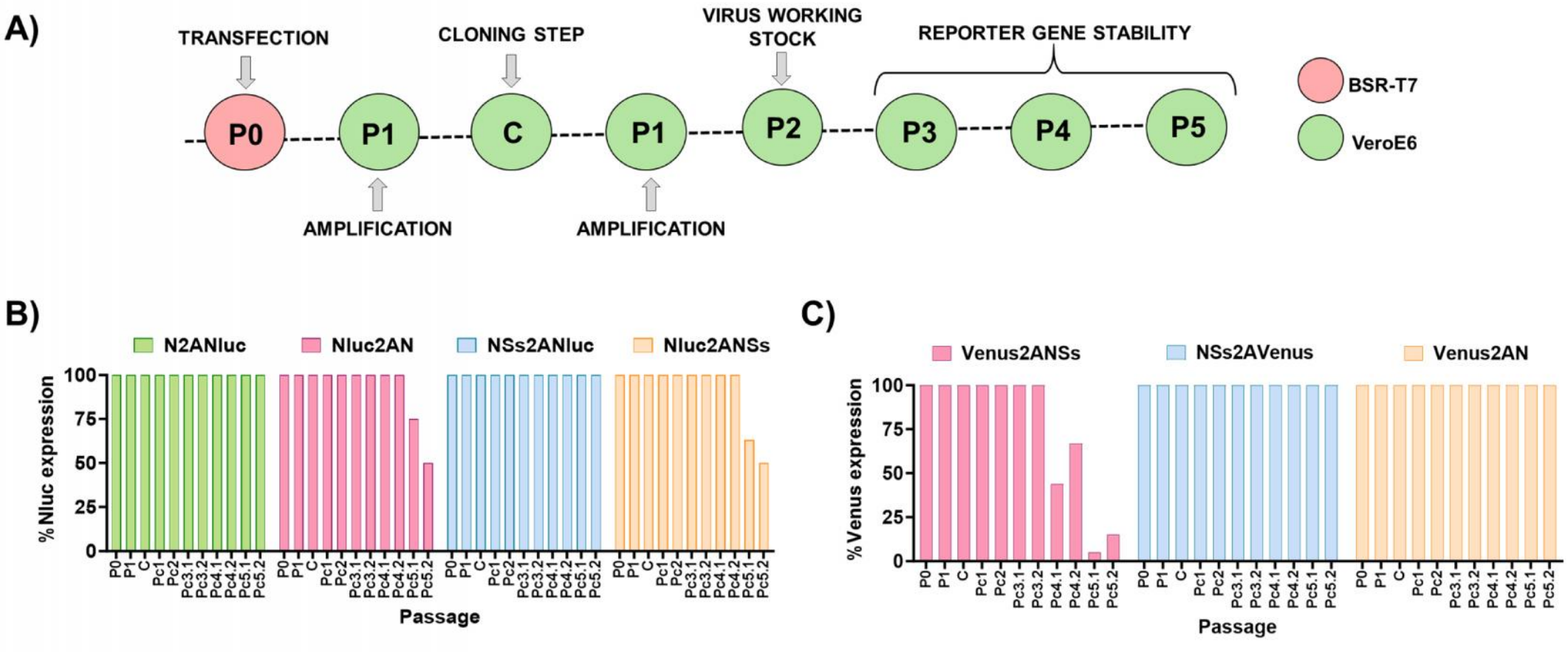
A)
TRANSFECTION
CLONING STEP
VIRUS WORKING STOCK
REPORTER GENE STABILITY
P0
P1
C
P1
P2
P3
P4
P5
AMPLIFICATION
AMPLIFICATION
BSR-T7
VeroE6
B)
N2ANluc
Nluc2AN
NSs2ANluc
Nluc2ANSs
% Nluc expression
Passage
C)
Venus2ANSs
NSs2AVenus
Venus2AN
% Venus expression
Passage

Figure 8

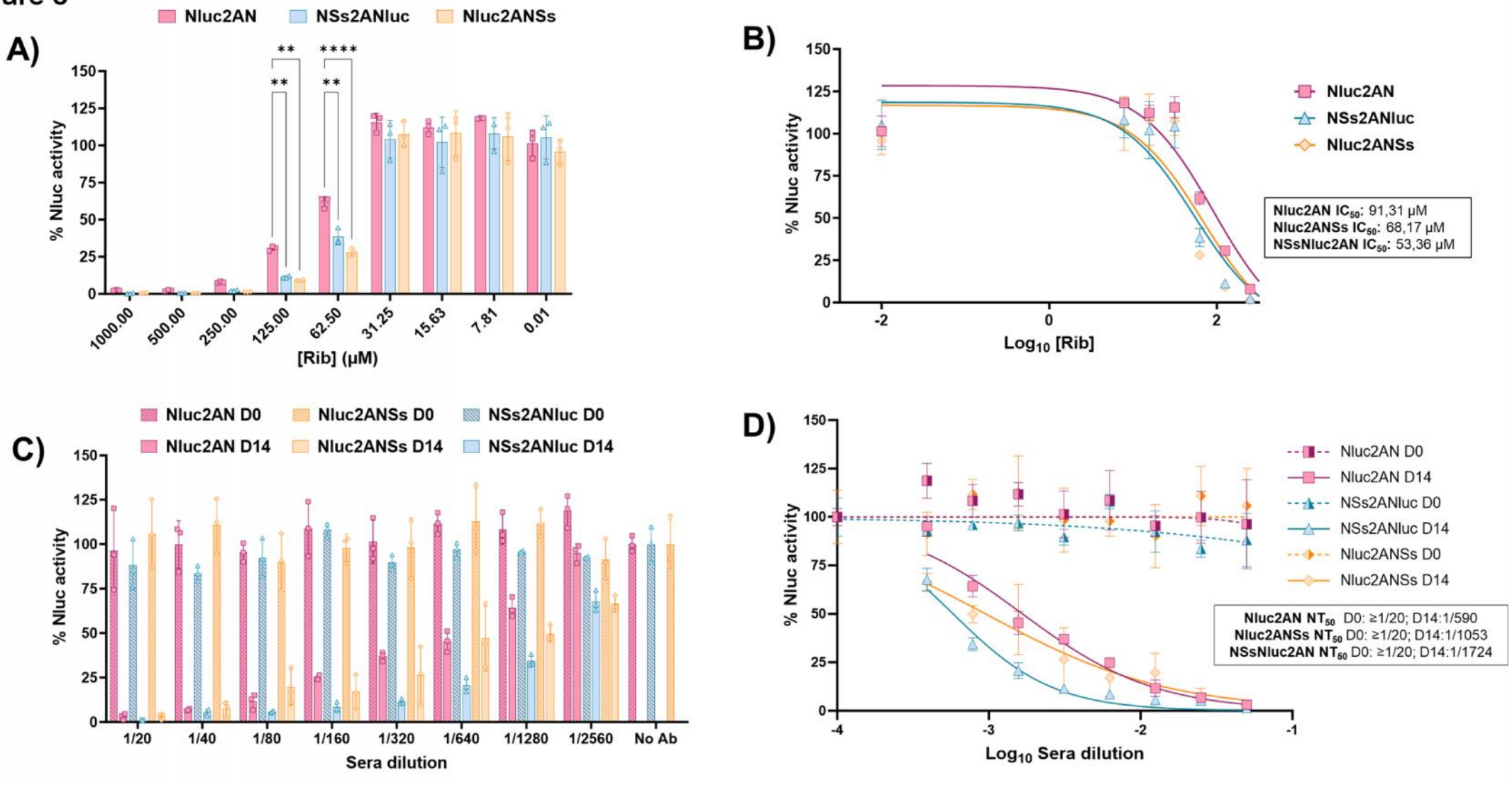
A)
Nluc2AN
NSs2ANluc
Nluc2ANSs
% Nluc activity
[Rib] (μM)
1000.00
500.00
250.00
125.00
62.50
31.25
15.63
7.81
0.01
B)
Nluc2AN
NSs2ANluc
Nluc2ANSs
Nluc2AN IC50: 91,31 μM
Nluc2ANSs IC50: 68,17 μM
NSsNluc2AN IC50: 53,36 μM
% Nluc activity
Log10 [Rib]
C)
Nluc2AN D0
Nluc2ANSs D0
NSs2ANluc D0
Nluc2AN D14
Nluc2ANSs D14
NSs2ANluc D14
% Nluc activity
1/20
1/40
1/80
1/160
1/320
1/640
1/1280
1/2560
No Ab
Sera dilution
D)
Nluc2AN D0
Nluc2AN D14
NSs2ANluc D0
NSs2ANluc D14
Nluc2ANSs D0
Nluc2ANSs D14
Nluc2AN NT50 D0: ≥1/20; D14:1/590
Nluc2ANSs NT50 D0: ≥1/20; D14:1/1053
NSsNluc2AN NT50 D0: ≥1/20; D14:1/1724
% Nluc activity
Log10 Sera dilution

Figure 9

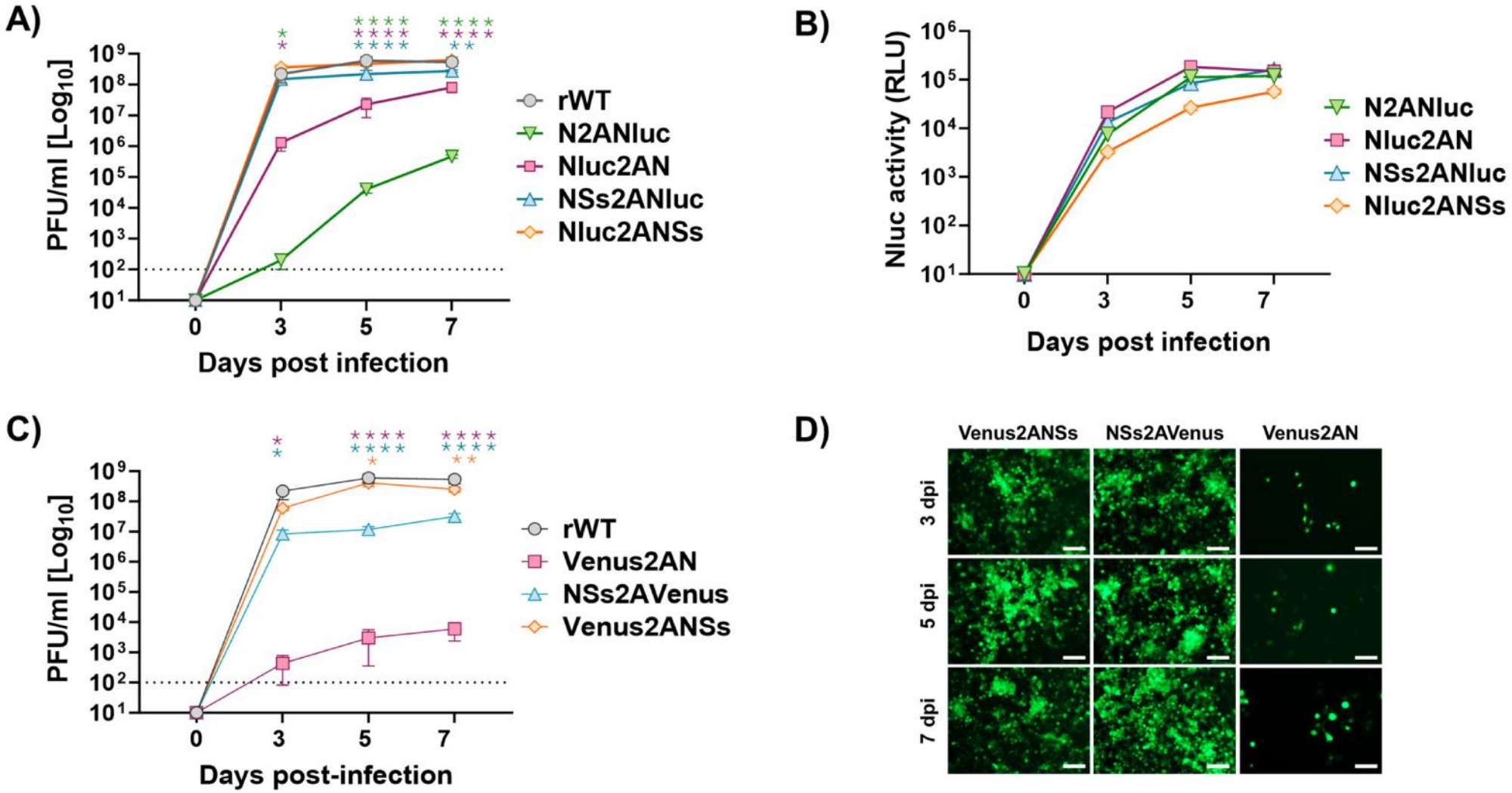
A)
PFU/ml [Log10]
Days post infection
rWT
N2ANluc
Nluc2AN
NSs2ANluc
Nluc2ANSs
B)
Nluc activity (RLU)
Days post infection
N2ANluc
Nluc2AN
NSs2ANluc
Nluc2ANSs
C)
PFU/ml [Log10]
Days post-infection
rWT
Venus2AN
NSs2AVenus
Venus2ANSs
D)
Venus2ANSs
NSs2AVenus
Venus2AN
3 dpi
5 dpi
7 dpi

Figure 10

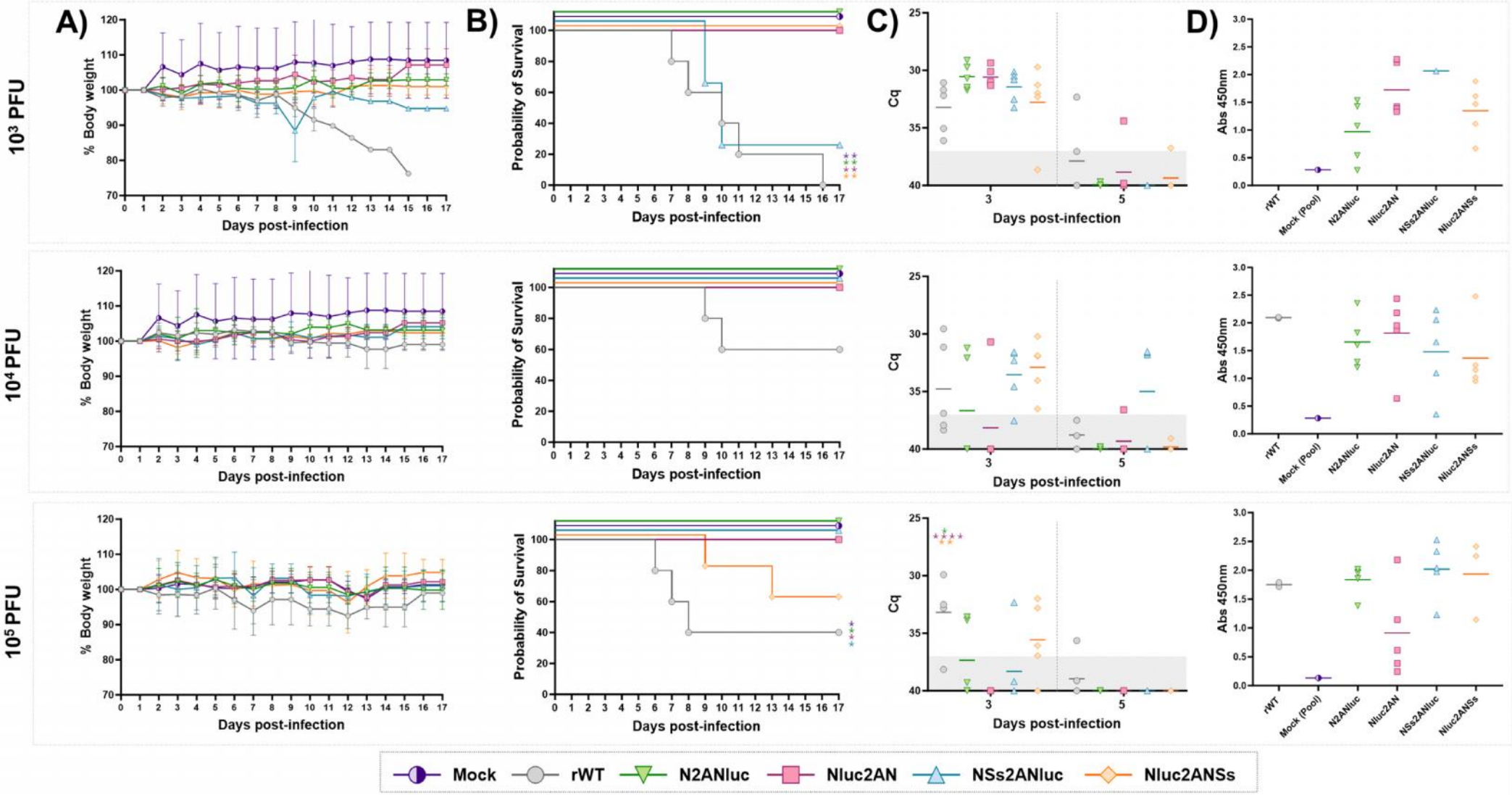
A)
B)
C)
D)
10³ PFU
10⁴ PFU
10⁵ PFU
% Body weight
Probability of Survival
Cq
Abs 450nm
Days post-infection
rWT
Mock (Pool)
N2ANluc
Nluc2AN
NSs2ANluc
Nluc2ANSs
Mock
rWT
N2ANluc
Nluc2AN
NSs2ANluc
Nluc2ANSs